X-ray Photodynamics

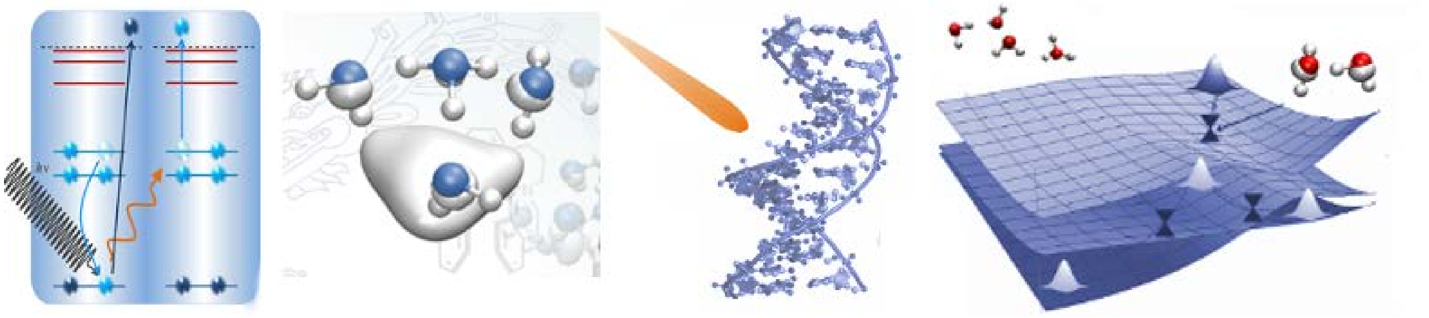

Petr Slavíček

Department of Physical Chemistry, University of Chemistry and Technology, Prague
and
Jaroslav Heyrovský Institute of Physical Chemistry, Academy of Sciences of the Czech Republic

Computational Photodynamics

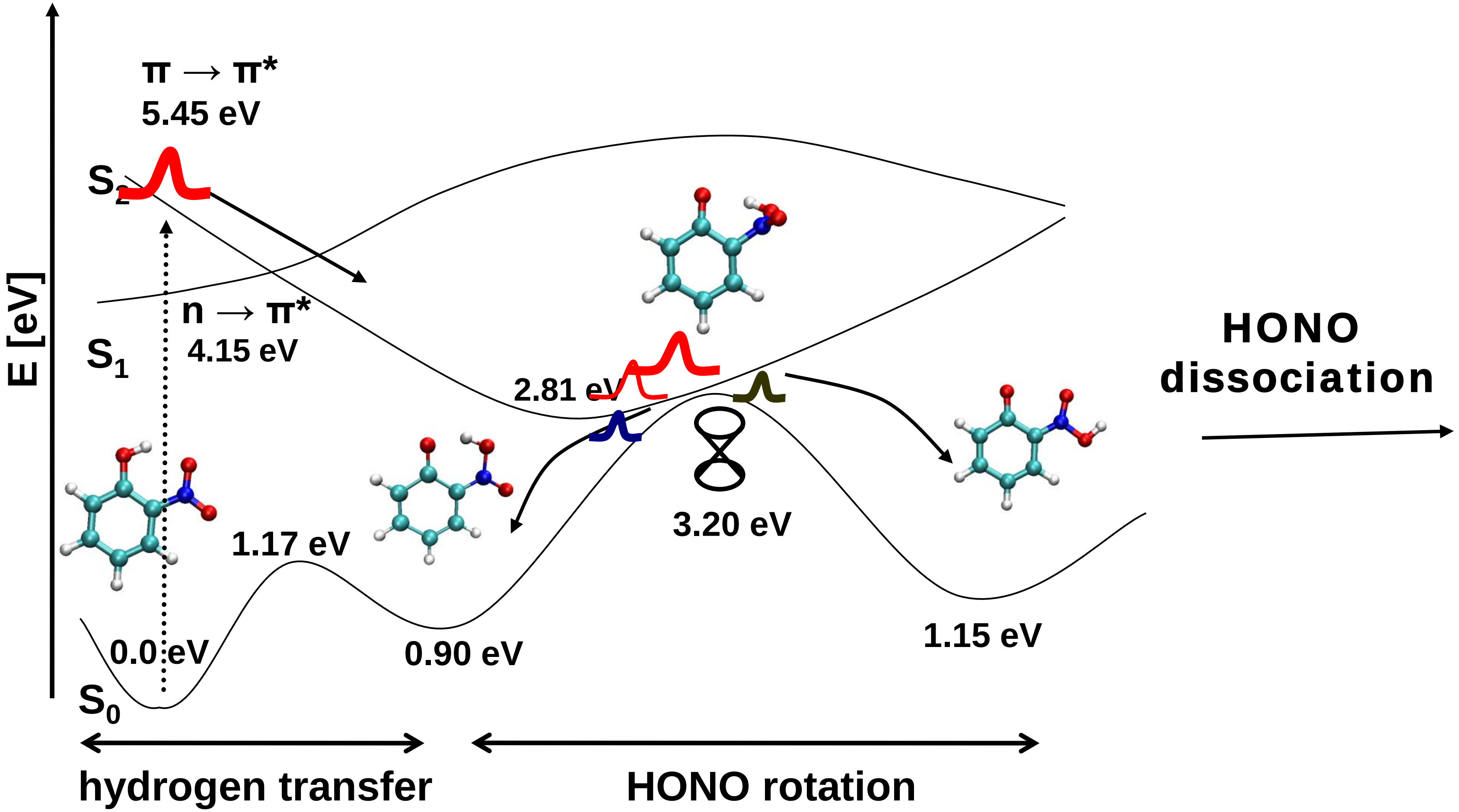

(SA3-6/5 MRCI / 6-31g*, dynamics at CASSCF level)

X-ray Photons Probing UV Photodynamics

$$\boxed{2Fe^{III}(C_2O_4)_3{}^{3-}} \longrightarrow \boxed{?} \longrightarrow \boxed{\begin{array}{c}2Fe^{II}(C_2O_4)_2{}^{2-}\\ +2CO_2 + C_2O_4{}^{2-}\end{array}}$$

Possible mechanisms:

1. $[Fe^{III}(C_2O_4)_3]^{3-} \xrightarrow{h\upsilon} [Fe^{III}(C_2O_4)_3{}^{3-}]^* \rightarrow [(\bullet\, C_2O_4)Fe^{II}\,(C_2O_4)_2]^{3-}$
2. $[Fe^{III}(C_2O_4)_3]^{3-} \xrightarrow{h\upsilon} [Fe^{III}(C_2O_4)_3{}^{3-}]^* \rightarrow [Fe^{III}(C_2O_4)_3]^{2-} + e_{solv}$
3. $[Fe^{III}(C_2O_4)_3]^{3-} \xrightarrow{h\upsilon} [Fe^{III}(C_2O_4)_3{}^{3-}]^* \rightarrow [Fe^{III}(C_2O_4)_2]^{-} + 2CO_2{}^{\bullet -}$
4. $[Fe^{III}(C_2O_4)_3]^{3-}\left(S=\frac{5}{2}\right) \xrightarrow{h\upsilon} [Fe^{III}(C_2O_4)_3{}^{3-}]^*\left(S=\frac{5}{2}\right) \rightarrow [Fe^{III}(C_2O_4)_3]^{3-}\left(S=\frac{3}{2}\right)$
5. $[Fe^{III}(C_2O_4)_3]^{3-}\left(S=\frac{5}{2}\right) \xrightarrow{h\upsilon} [Fe^{III}(C_2O_4)_3{}^{3-}]^*\left(S=\frac{5}{2}\right) \rightarrow [Fe^{III}(C_2O_4)_3]^{3-}\left(S=\frac{1}{2}\right)$

small quantum yield

not very likely

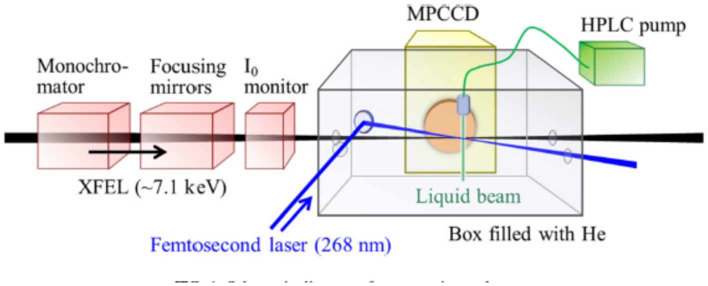

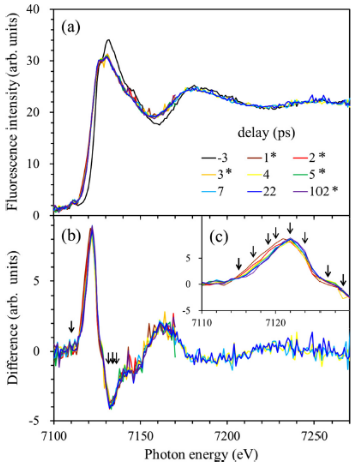

Struct. Dyn. 2, (2015), 034901.

Radiation Chemistry

The science of chemical effects brought about by the absorption of ionizing radiation in matter, mainly due to electronic processes (different from radiochemistry).

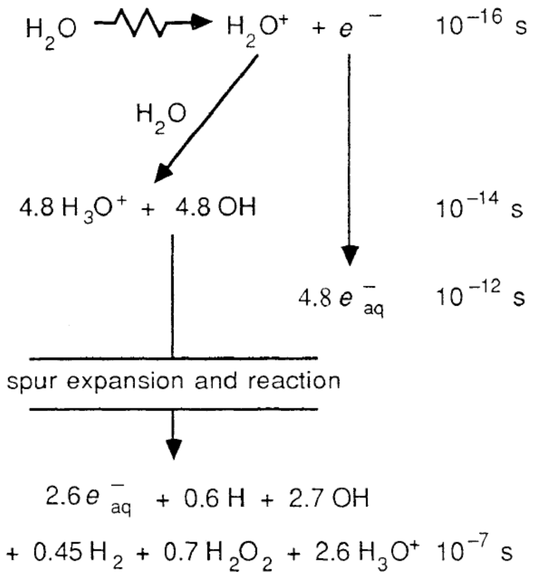

$\rightsquigarrow$ Under the action of ionizing radiation, without specification of mechanism

$$G = \frac{\text{Number of molecules}}{100\ eV}$$

X-rays: Radiation Damage

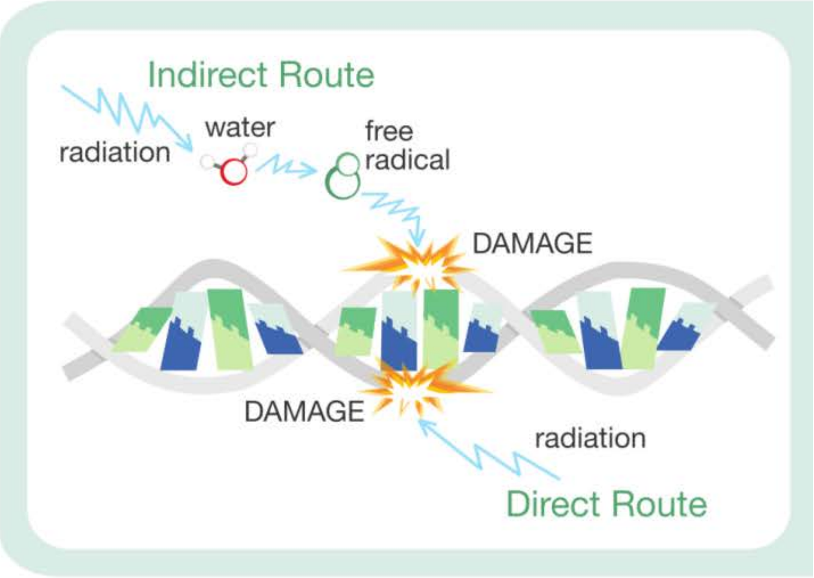

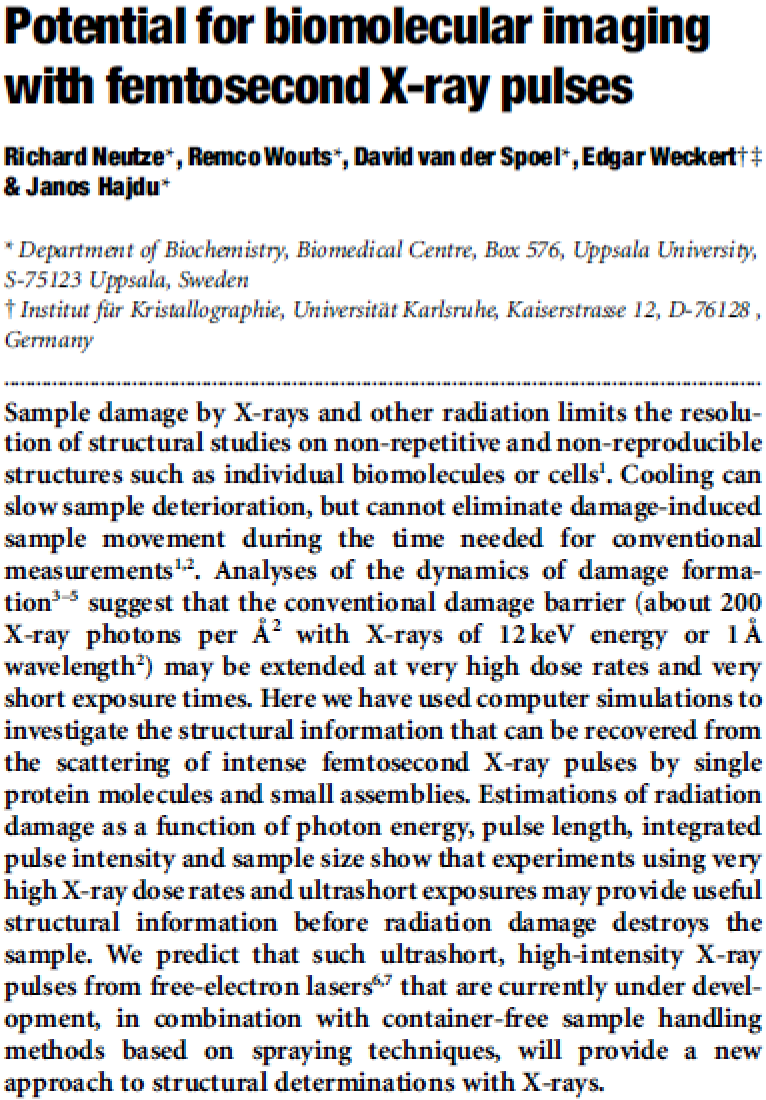

Potential for biomolecular imaging with femtosecond X-ray pulses

Richard Neutze*, Remco Wouts*, David van der Spoel*, Edgar Weckert†‡ & Janos Hajdu*

** Department of Biochemistry, Biomedical Centre, Box 576, Uppsala University, S-75123 Uppsala, Sweden*
† Institut für Kristallographie, Universität Karlsruhe, Kaiserstrasse 12, D-76128 , Germany

Sample damage by X-rays and other radiation limits the resolution of structural studies on non-repetitive and non-reproducible structures such as individual biomolecules or cells[1]. Cooling can slow sample deterioration, but cannot eliminate damage-induced sample movement during the time needed for conventional measurements[1,2]. Analyses of the dynamics of damage formation[3–5] suggest that the conventional damage barrier (about 200 X-ray photons per Å^2 with X-rays of 12 keV energy or 1 Å wavelength[2]) may be extended at very high dose rates and very short exposure times. Here we have used computer simulations to investigate the structural information that can be recovered from the scattering of intense femtosecond X-ray pulses by single protein molecules and small assemblies. Estimations of radiation damage as a function of photon energy, pulse length, integrated pulse intensity and sample size show that experiments using very high X-ray dose rates and ultrashort exposures may provide useful structural information before radiation damage destroys the sample. We predict that such ultrashort, high-intensity X-ray pulses from free-electron lasers[6,7] that are currently under development, in combination with container-free sample handling methods based on spraying techniques, will provide a new approach to structural determinations with X-rays.

X-ray Photons as Reactants

Specific bond cleavage

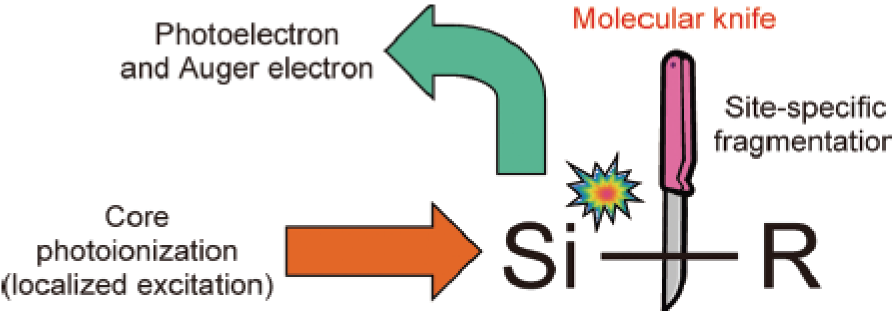

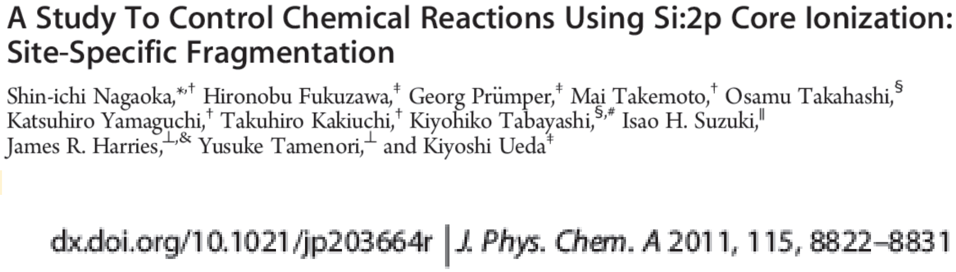

A Study To Control Chemical Reactions Using Si:2p Core Ionization: Site-Specific Fragmentation

Shin-ichi Nagaoka,[*,†] Hironobu Fukuzawa,[‡] Georg Prümper,[‡] Mai Takemoto,[†] Osamu Takahashi,[§]
Katsuhiro Yamaguchi,[†] Takuhiro Kakiuchi,[†] Kiyohiko Tabayashi,[§,#] Isao H. Suzuki,[∥]
James R. Harries,[⊥,&] Yusuke Tamenori,[⊥] and Kiyoshi Ueda[‡]

dx.doi.org/10.1021/jp203664r | *J. Phys. Chem. A* 2011, 115, 8822–8831

Highly Selective Dissociation of a Peptide Bond Following Excitation of Core Electrons

Yi-Shiue Lin,[†,‡] Cheng-Cheng Tsai,[⊥] Huei-Ru Lin,[†,‡,§] Tsung-Lin Hsieh,[†,‡] Jien-Lian Chen,[‡,⊥]
Wei-Ping Hu,[*,⊥] Chi-Kung Ni,[*,‡,∥] and Chen-Lin Liu[*,†]

DOI: 10.1021/acs.jpca.5b04415
J. Phys. Chem. A 2015, 119, 6195−6202

X-ray Photons as Reactants

Radiosenzitization and activation of nanoparticles

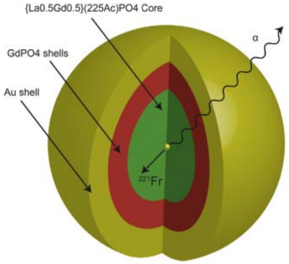

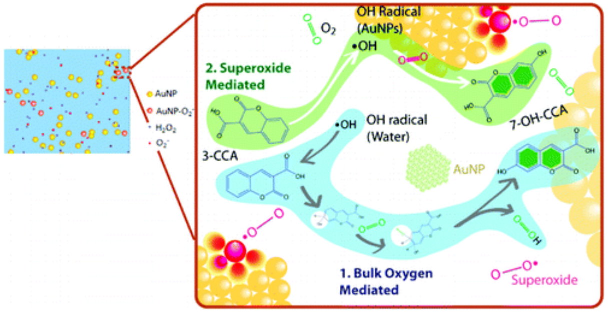

Formation of new species in astrochemical environments

X-ray photochromism

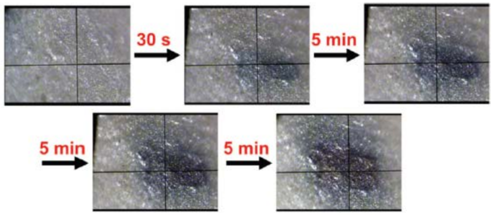

Figure 4. An X-ray-induced photochromic process of **1-Y**. The images were recorded in an X-ray photoelectron spectrometer (λ = 8.357 Å; powered at 150 W; spot size: 500 µm in diameter) using a tablet (0.8 mm in thickness) of powdered single crystals.

X-ray photoreduction

X-ray Photons as Reactants

X-ray uncaging

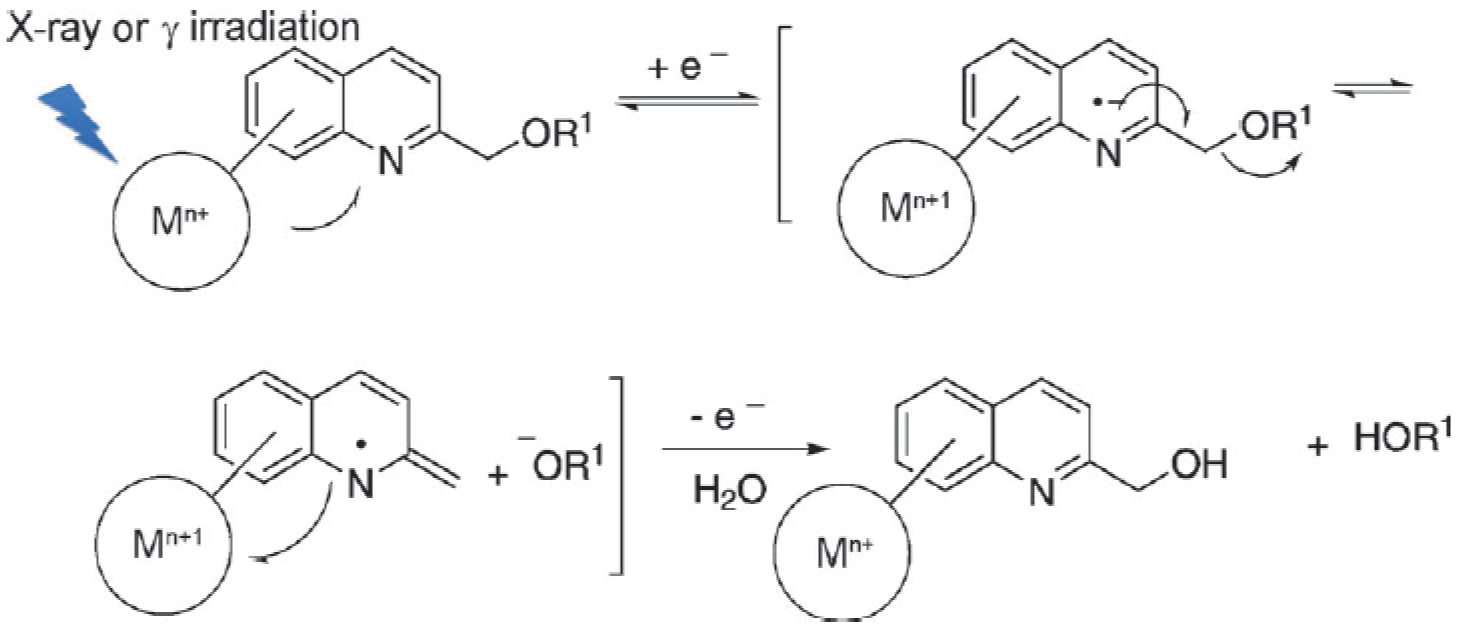

Scheme 1. Auger electron-mediated electron transfer (ET) leading to fragmentation of hydroxymethyl quinolines.

Angew. Chem. **2011**, *123*, 9882–9885

Understanding Spectroscopy

Isotope effects in XES

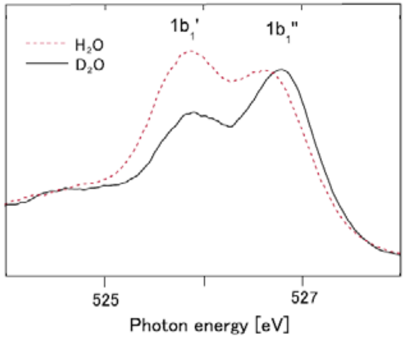

Fig. 5. Comparison of the D_2O and H_2O spectra in the $1b_1$ region at 7 °C. The spectra have been normalized to the same $1b_1''$ peak height.

T. Tokushima et al. / Chemical Physics Letters 460 (2008) 387–400

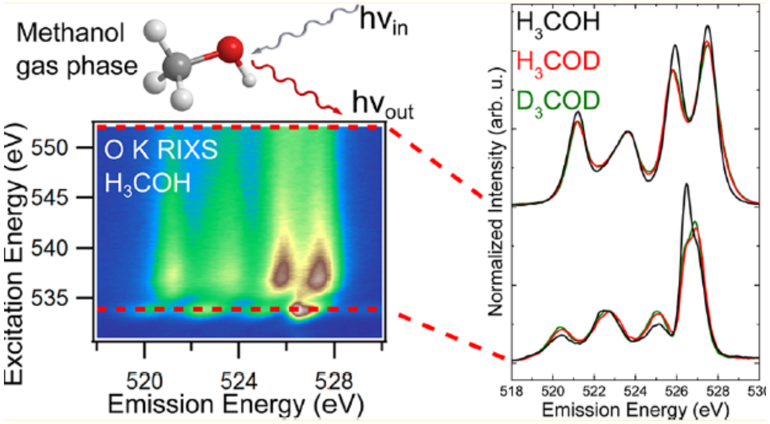

J. Phys. Chem. A 2016, 120, 2260–2267

Isotope effects in Auger

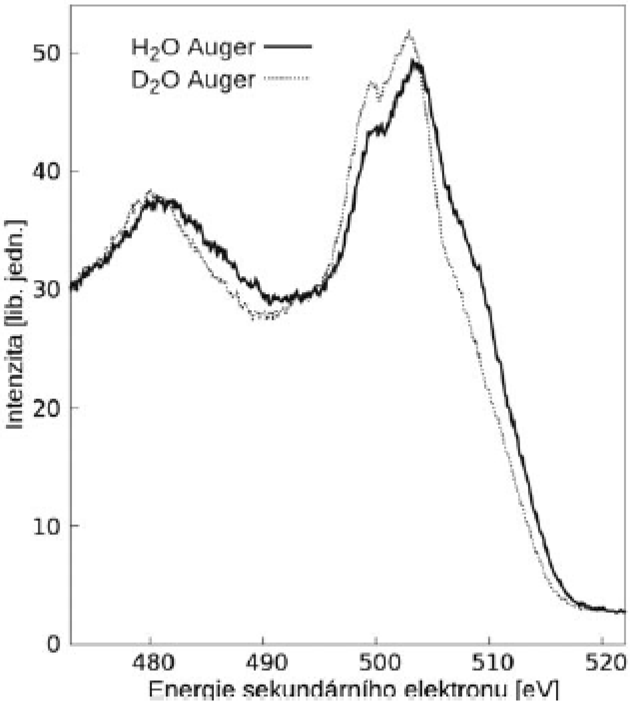

Molecules and Radiation

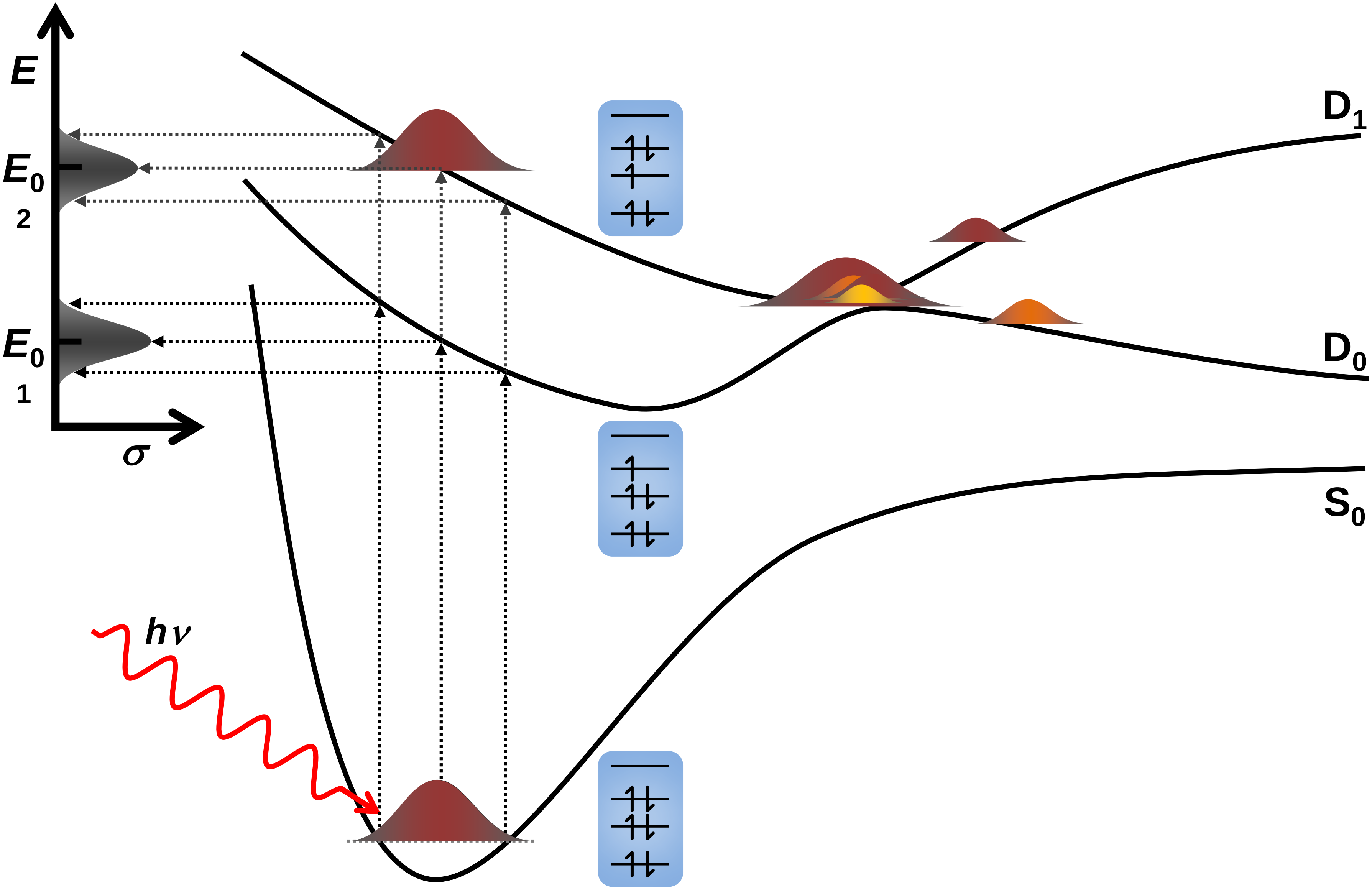

Molecules and High Energy Radiation

Large number of electronic states

New processes

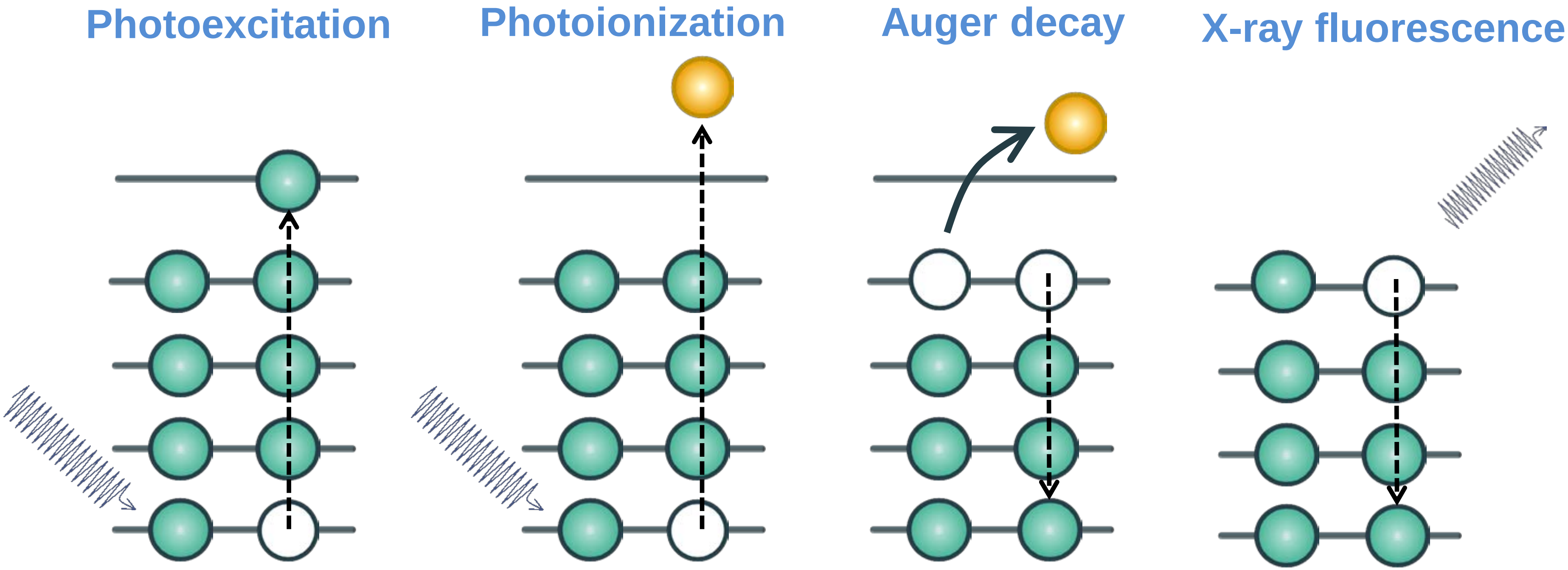

Photoexcitation

Photoionization

Auger decay

X-ray fluorescence

Molecules and High Energy Radiation

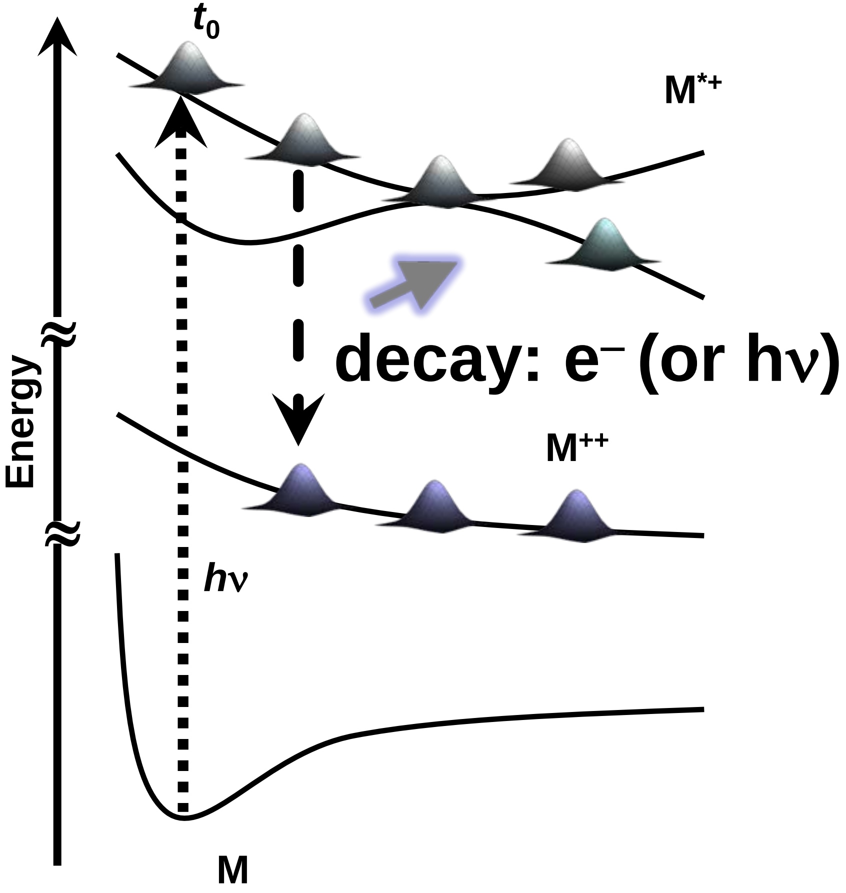

Absorption

Nuclear motion

Non-adiabatic transitions

Fluorescence

$$A_{if} = \frac{64\pi\nu^3}{4\pi\varepsilon_0 3hc^3}\left|\vec{\mu}_{if}\right|^2$$

Autoionization

Secondary Processes: The Main Channel

Primary versus secondary processes in water

Auger Cascade

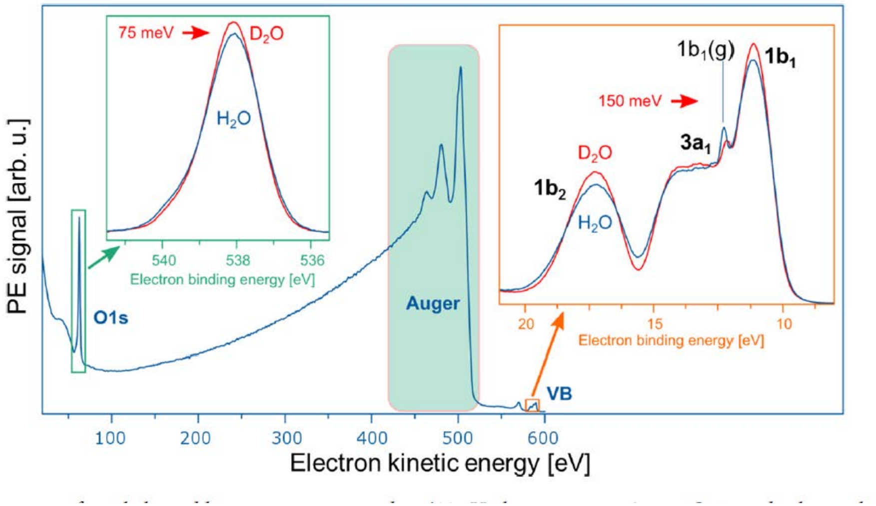

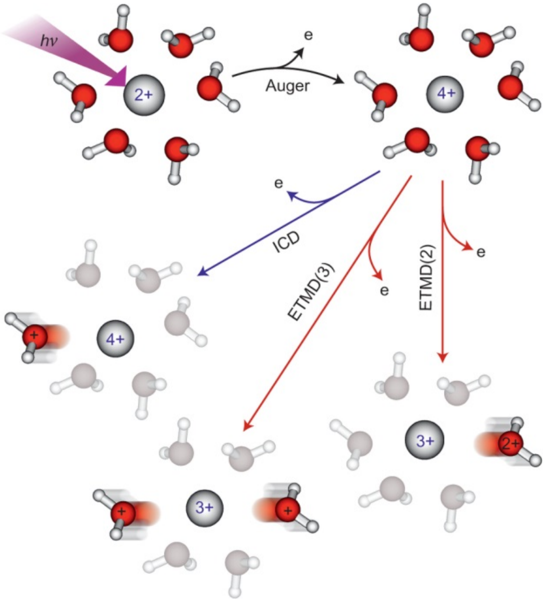

Slavicek, Kryzhevoi, Aziz, WinterJ. *Phys. Chem. Lett.*, 7 , 234–243 (2016)

Stupmf, Gokhberg, Cederbaum *Nature Chemistry* 8, 237–241 (2016)

Exact Solution of Schrodinger Equation

$$i\frac{\partial\Psi\left(\vec{r},\vec{R},t\right)}{\partial t}=\left(\hat{T}\left(\vec{r},\vec{R}\right)+\hat{V}_{Coulomb}\left(\vec{r},\vec{R}\right)\right)\Psi\left(\vec{r},\vec{R},t\right)$$

Limitations to several particles (including electrons)

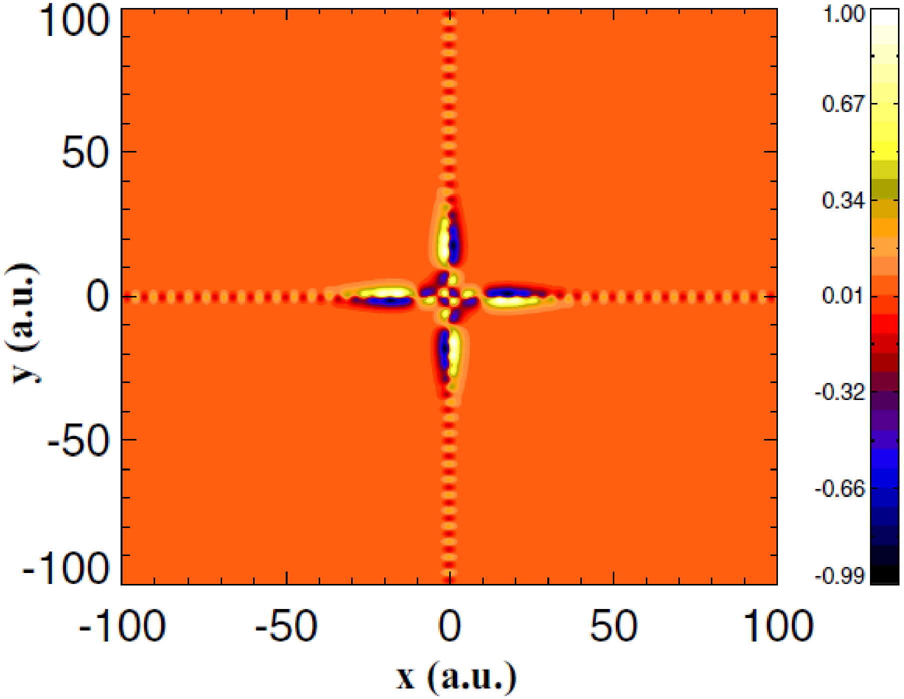

PHYSICAL REVIEW A **93**, 063408 (2016)

Solving Problem Step by Step

Promoting molecule into excited state

Time evolution on single PES

Population transfer between electronic states

Coupling to continuum

Follow up dynamic

Quantum (Adiabatic) Dynamics

Born-Oppenheimer approximation

$$\Psi^T(\mathbf{r},\mathbf{R},t) = \chi_I(\mathbf{R},t)\Psi_I^e(\mathbf{r};\mathbf{R})$$

Potential Energy Surface

$$H^e\Psi_I^e = E_I^e(R)\Psi_I^e$$

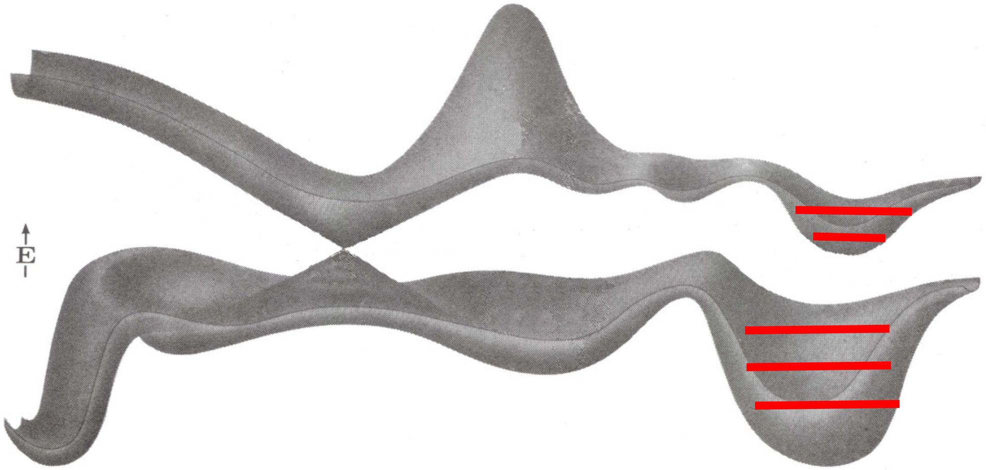

Calculating vibrational states

$$(T^N + E_I^e)\chi_I = E^T\chi_I$$

Wavepacket evolution

$$(T^N + E_I^e(R))\chi_I(R,t) =$$

$$i\frac{\partial}{\partial t}\chi_I(R,t)$$

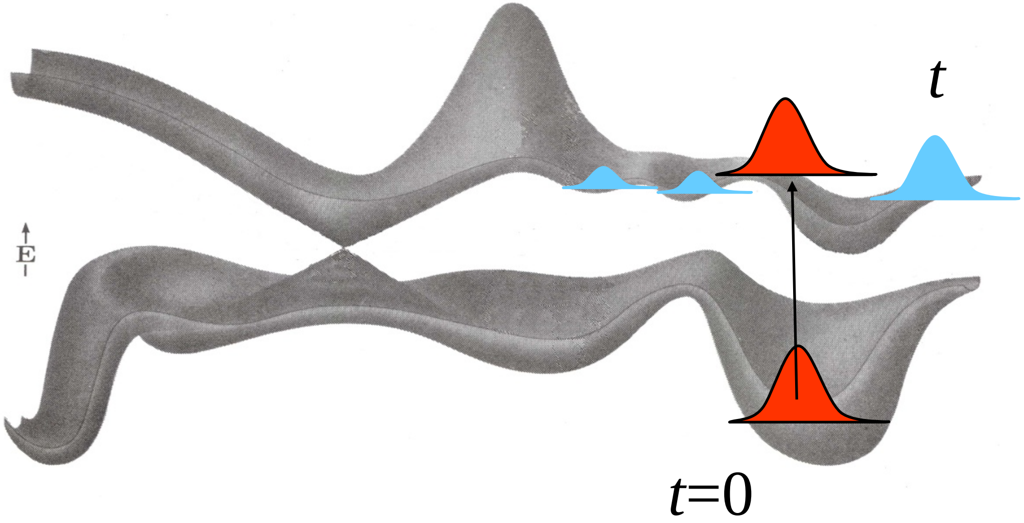

Quantum and Classical (Adiabatic) Dynamics

Quantum Dynamics

$$i\hbar \frac{\partial \chi}{\partial t} = \hat{H}\chi \qquad \hat{H} = \hat{T} + E_I^e(\boldsymbol{R})$$

Solving by e.g. expansion into a basis

$$\chi(t) = \sum_n A_n(t)\phi_n \qquad i\hbar \frac{\partial A_n(t)}{\partial t} = \sum_m H_{nm}A_m(t)$$

Classical dynamics approximates quantum dynamics

$$\frac{\mathrm{d}\boldsymbol{R}}{\mathrm{d}t} = \frac{\boldsymbol{P}}{m}$$

We need (initial) positions and momenta!

$$\frac{\mathrm{d}\mathbf{P}}{\mathrm{d}t} = -\frac{\mathrm{d}E_\mathrm{I}^\mathrm{e}(\boldsymbol{R})}{d\boldsymbol{R}}$$

Quasiclassical Approach: Wigner distribution

Wigner distribution function, definition

$$\rho_w(x,p,t)=\frac{1}{\pi\hbar}\int_{-\infty}^{\infty}\psi(x+y,t)^*\psi(x-y,t)e^{\frac{2ipy}{\hbar}}\,\mathrm{d}y$$

$$\rho_w(x,p,t)=\frac{1}{\pi\hbar}\int_{-\infty}^{\infty}\Phi(p+q,t)^*\Phi(p-q,t)e^{\frac{-2iqx}{\hbar}}\,\mathrm{d}q$$

Properties of Wigner distribution function

1. It is a real function

2. $$\int_{-\infty}^{\infty}\rho_w(x,p,t)\mathrm{d}p=\left|\psi(x,t)\right|^2$$
   $$\int_{-\infty}^{\infty}\rho_w(x,p,t)\mathrm{d}x=\left|\Phi(p,t)\right|^2$$

3. $$\int_{-\infty}^{\infty}\rho_w^{\chi}(x,p,t)\rho_w^{\psi}(x,p,t)\mathrm{d}x\mathrm{d}p=\langle\chi\,|\,\psi\rangle$$

It almost behaves as a probability distribution function …..however, WD can be negative

Positive distributions exist (Husimi)

Quasiclassical Approach: Wigner distribution

Equation of motion for the Wigner distribution

$$\frac{\partial \rho_W}{\partial t} = -\frac{p}{m}\frac{\partial \rho_W}{\partial q} + V'(q)\frac{\partial \rho_W}{\partial p} - \frac{\hbar^2}{24}V'''(q)\frac{\partial^3 \rho_W}{\partial p^3} + \cdots$$

From which we can derive underlying “Hamilton” equations

$$\dot{q} = v_q = \frac{p}{m},$$

$$\dot{p} = v_p = -V'(q) + \frac{\hbar^2}{24}V'''(q)\frac{1}{\rho}\frac{\partial^2 \rho}{\partial p^2} + \cdots$$

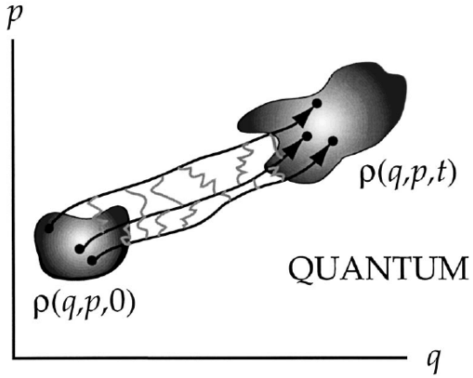

Hamilton function is no more a constant along the trajectory

$$\frac{dH}{dt} = \dot{q}\frac{\partial H}{\partial q} + \dot{p}\frac{\partial H}{\partial p} = \frac{p}{m}\left(\frac{\hbar^2}{24}V'''(q)\frac{1}{\rho}\frac{\partial^2 \rho}{\partial p^2} + \cdots\right)$$

Semiclassical Description: Wavepacket Dispersion

1D quantum description vs. fully dimensional semiclassical description

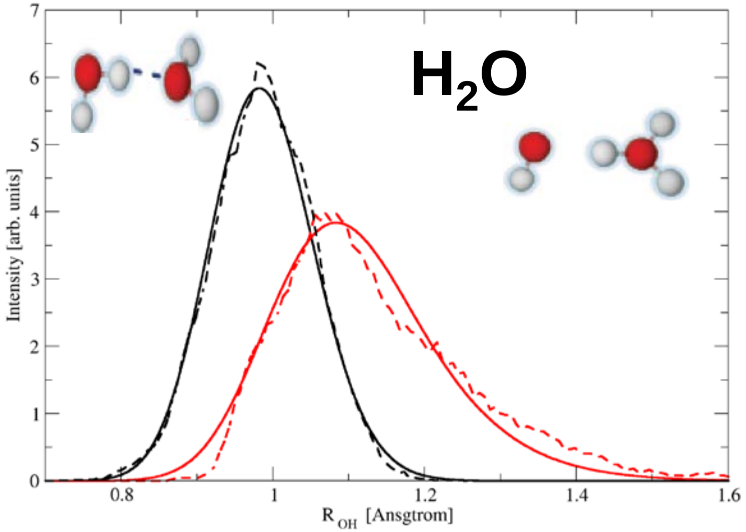

The process is essentially 1D in this case

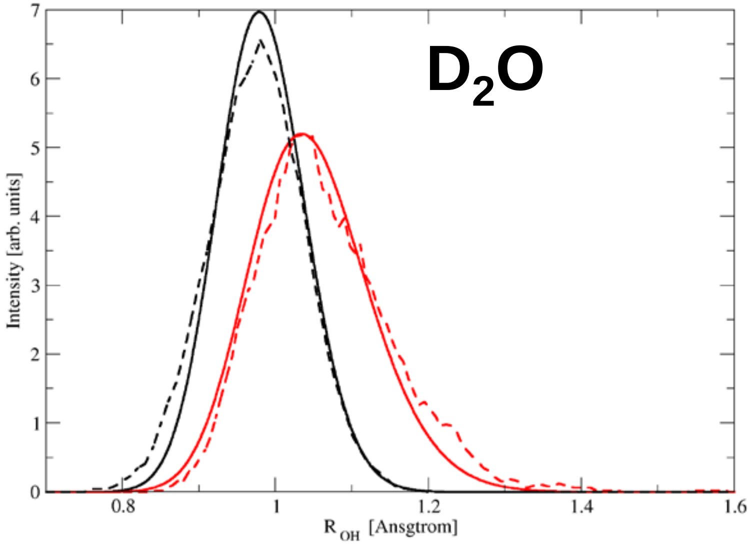

How to Get Potential Energy Surface?

Low-lying excited states

Whole plethora of available methods

Variational collapse for highly excited states

Selecting proper states e.g. by Maximum Overlap Method

Preselected excitations

RAS-SCF method, TDDFT approach…

Thrifty solution: *Z*+1 method

Simulating (slightly) different system

Beyond Born-Oppenheimer

$$\Psi^T(\mathbf{r},\mathbf{R}) = \sum_{I=1}^{N^a} \chi_I(\mathbf{R})\Psi_I^e(\mathbf{r};\mathbf{R})$$

If the expansion is not truncated the wavefunction is exact since the set Ψ_I^e is complete.

$$(T^N + \frac{1}{\mu}K^{II} + E_I^e)\chi_I + \sum_{J\neq I}^{N}\frac{1}{2\mu}(-2\mathbf{f}^{IJ}\cdot\nabla\chi_J + K^{IJ}\chi_J) = i\frac{\partial}{\partial t}\chi_I$$

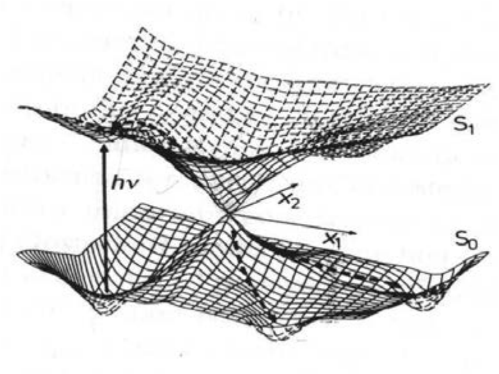

$$f_\alpha^{IJ}(\mathbf{R}) = \left\langle \Psi_I^e \middle| \nabla_\alpha \Psi_J^e \right\rangle_{\mathbf{r}}$$

$$k^{IJ}(\mathbf{R}) = \left\langle \Psi_I^e \middle| \nabla^2 \Psi_J^e \right\rangle_{\mathbf{r}}$$

Derivative couplings connects the different electronic states

Beyond Born-Oppenheimer

$$\boldsymbol{f}_{\alpha}^{IJ} = \langle \psi_I^e | \nabla_\alpha | \psi_J^e \rangle = \frac{\langle \psi_I^e | \nabla_\alpha \widehat{H}_e | \psi_J^e \rangle}{E_J - E_I}$$

$$\boldsymbol{f}_{\alpha}^{IJ} = -\boldsymbol{f}_{\alpha}^{JI}$$

$\boldsymbol{f}_{\alpha}^{II} = 0$ ← For real wavefunctions

The derivative coupling is inversely proportional to the energy difference of the two electronic states. Thus the smaller the difference, the larger the coupling. If *ΔE=0 f* is infinity.

Semiclassical Approach: Surface Hopping

With know trajectory *R*(*t*), at each point, we solve electron SE

$$\widehat{H}_e \emptyset_k(\boldsymbol{r}, \boldsymbol{R}(t)) = E_k(R(t))\emptyset_k(\boldsymbol{r}, \boldsymbol{R}(t))$$

The total wavefunction can then be expanded

$$\Psi(\mathbf{r}, \mathbf{R}, t) = \sum_{k=1}^{N_S} c_k(t)\phi_k(\mathbf{r}, \mathbf{R}(t))$$

Solving TDSE

$$\frac{dc_k(t)}{dt} = -i\hbar^{-1}E_k(t) - \sum c_j(t)\mathbf{F}_{kj}^c(R(t)) \cdot \mathbf{v}^c(t)$$

Random hops reflecting the electronic population

$$P_{l\to k} = \max\left[0, -\frac{2\Delta t}{c_l c_l^*}\mathrm{Re}\left(c_l c_k^*\right)\mathbf{F}_{kl}^c \cdot \mathbf{v}^c\right]$$

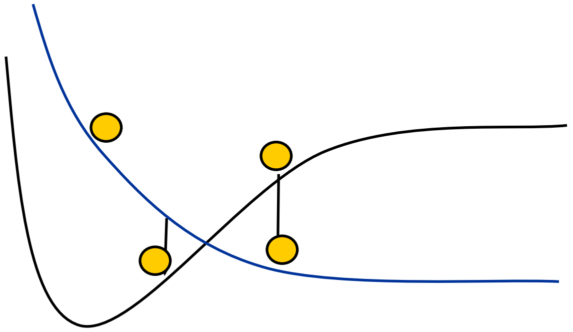

Semiclassical Approach: Surface Hopping

- Quantum nucleus

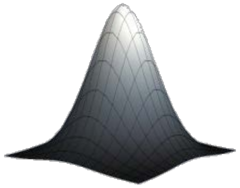

Classical approximation

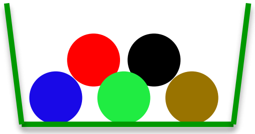

Classical nuclei

Swarm of trajectories

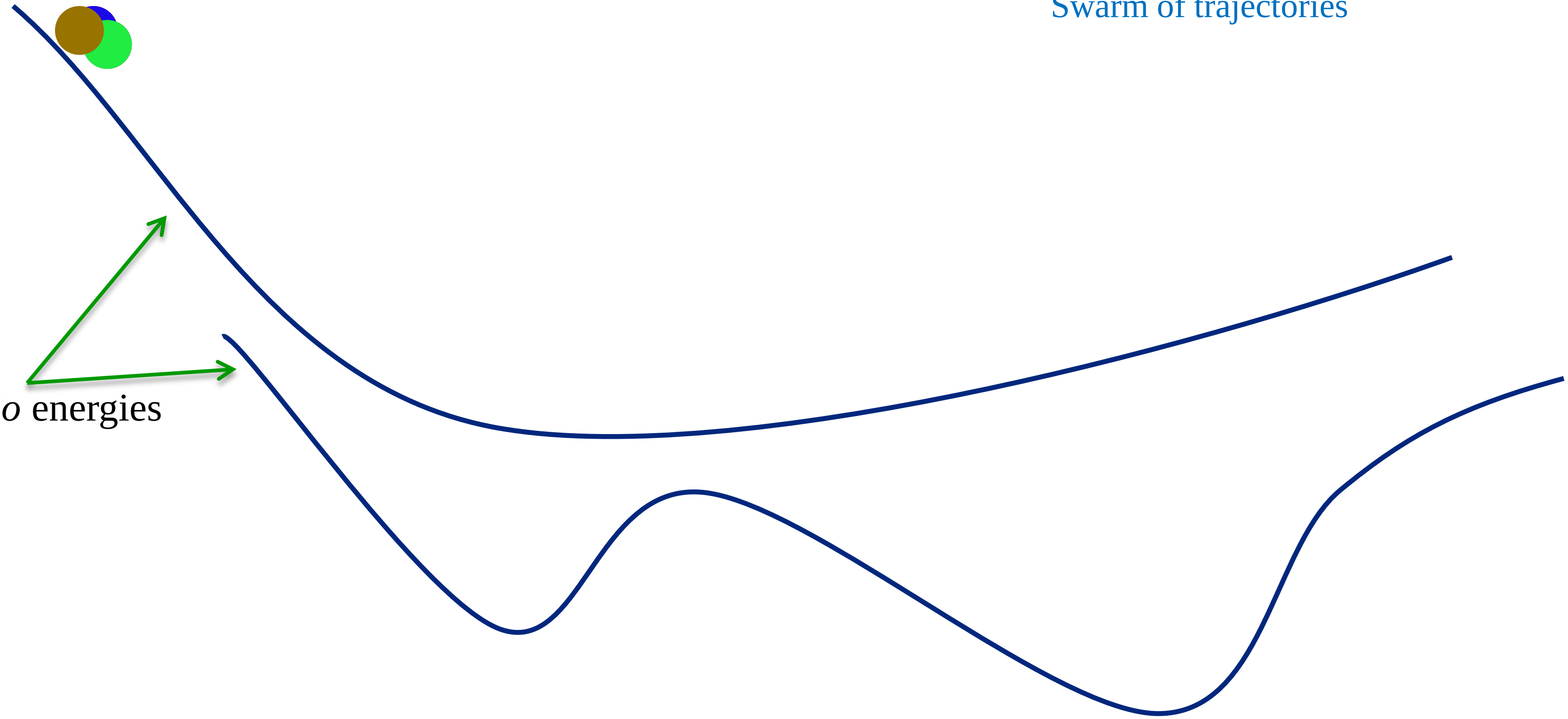

Ab initio energies

Statistical evaluation!

Semiclassical Approach: Ehrenfest method

With know trajectory *R*(*t*), at each point, we solve electron SE

$$\hat{H}_e \emptyset_k(\boldsymbol{r}, \boldsymbol{R}(t)) = E_k(R(t))\emptyset_k(\boldsymbol{r}, \boldsymbol{R}(t))$$

The total wavefunction can then be expanded

$$\Psi(\mathbf{r}, \mathbf{R}, t) = \sum_{k=1}^{N_S} c_k(t)\phi_k(\mathbf{r}, \mathbf{R}(t))$$

Solving TDSE

$$\frac{dc_k(t)}{dt} = -i\hbar^{-1}E_k(t) - \sum c_j(t)\mathbf{F}_{kj}^c(R(t)) \cdot \mathbf{v}^c(t)$$

Moving on average potential

$$V_{Ave} = \sum_k \phi_k^2 E_k$$

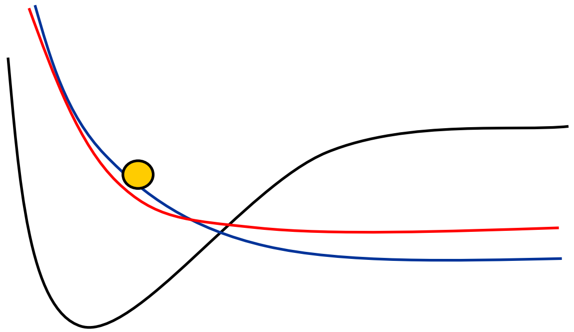

Example: Water Ionization

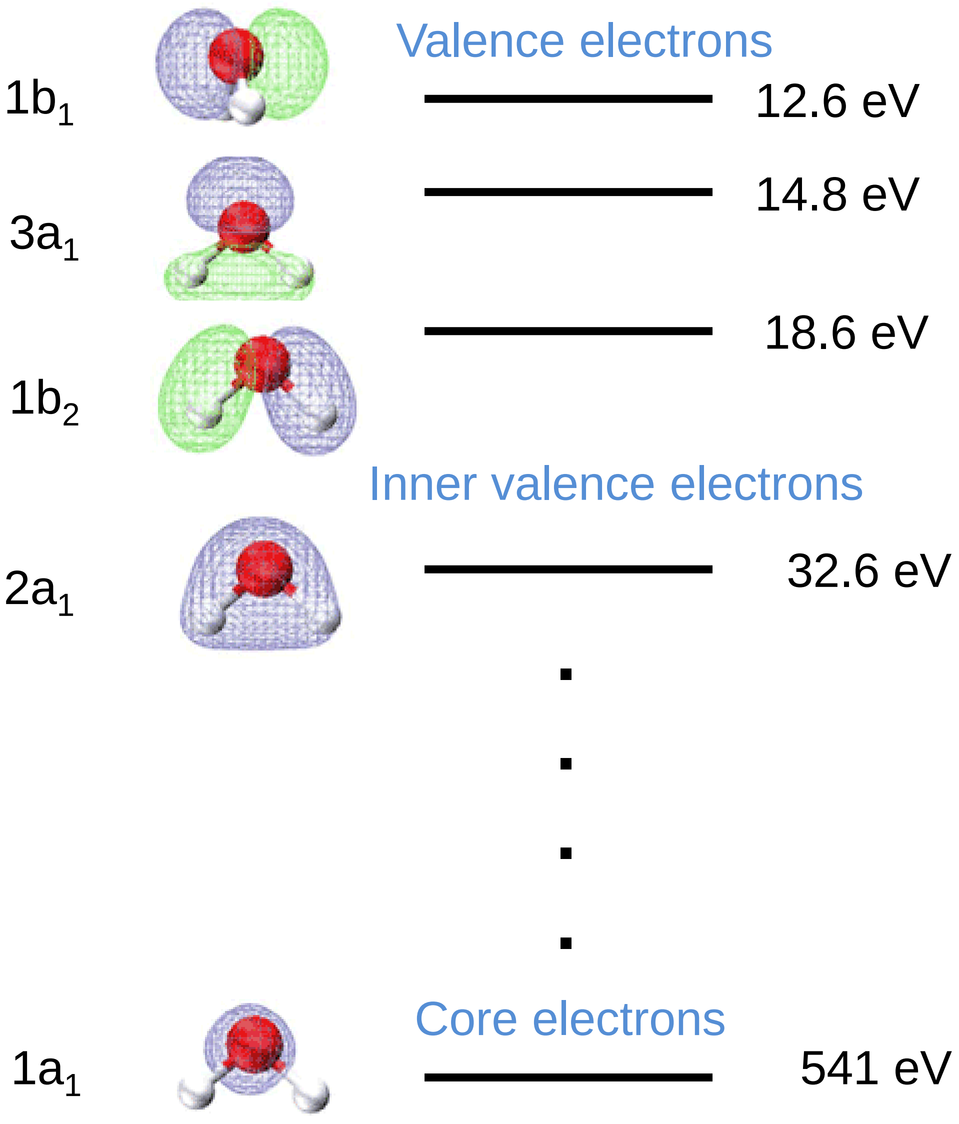

Valence electrons

$1b_1$ 12.6 eV

$3a_1$ 14.8 eV

$1b_2$ 18.6 eV

Inner valence electrons

$2a_1$ 32.6 eV

Core electrons

$1a_1$ 541 eV

Example: Water Ionization

Inspection of PES

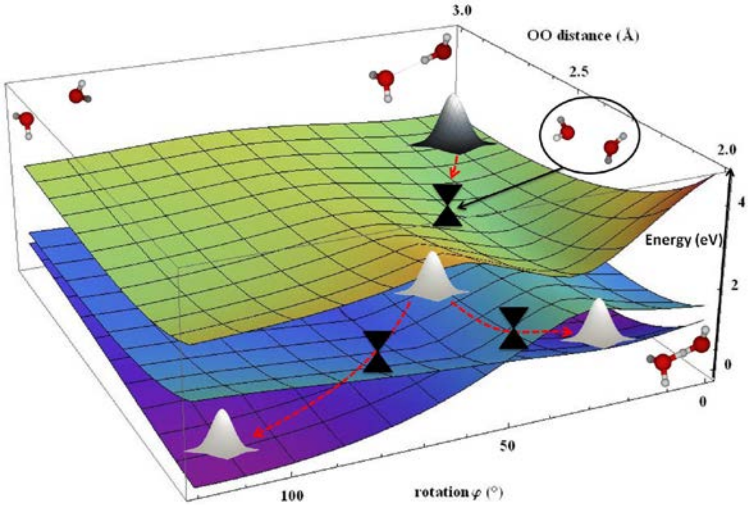

MD simulation

$$(H_2O)_2 \xrightarrow{3a_1} H_3O^+ + OH\bullet$$

$$(H_2O)_2 \xrightarrow{3a_1} H_2O^+ + H_2O$$

Initial state: D_2

Initial state: D_3

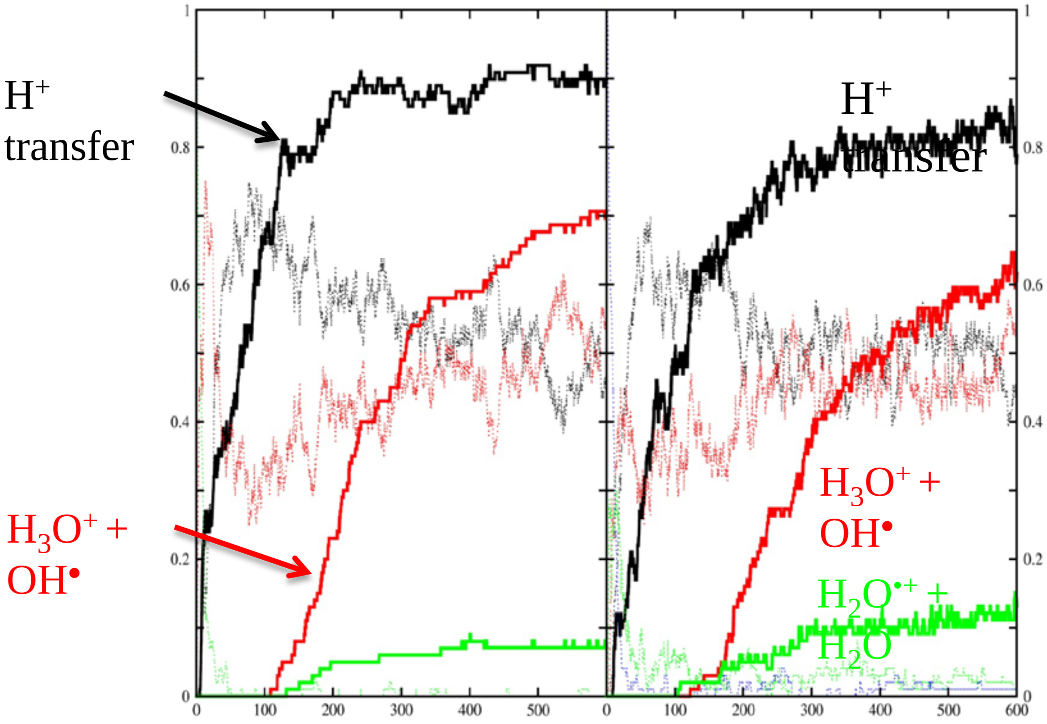

DONOR

ACCEPTOR

Svoboda, Hollas, Ončák, Slavíček, PhysChemChemPhys. 15 (2013) 11531.

Example: Water Ionization

Different reaction channels

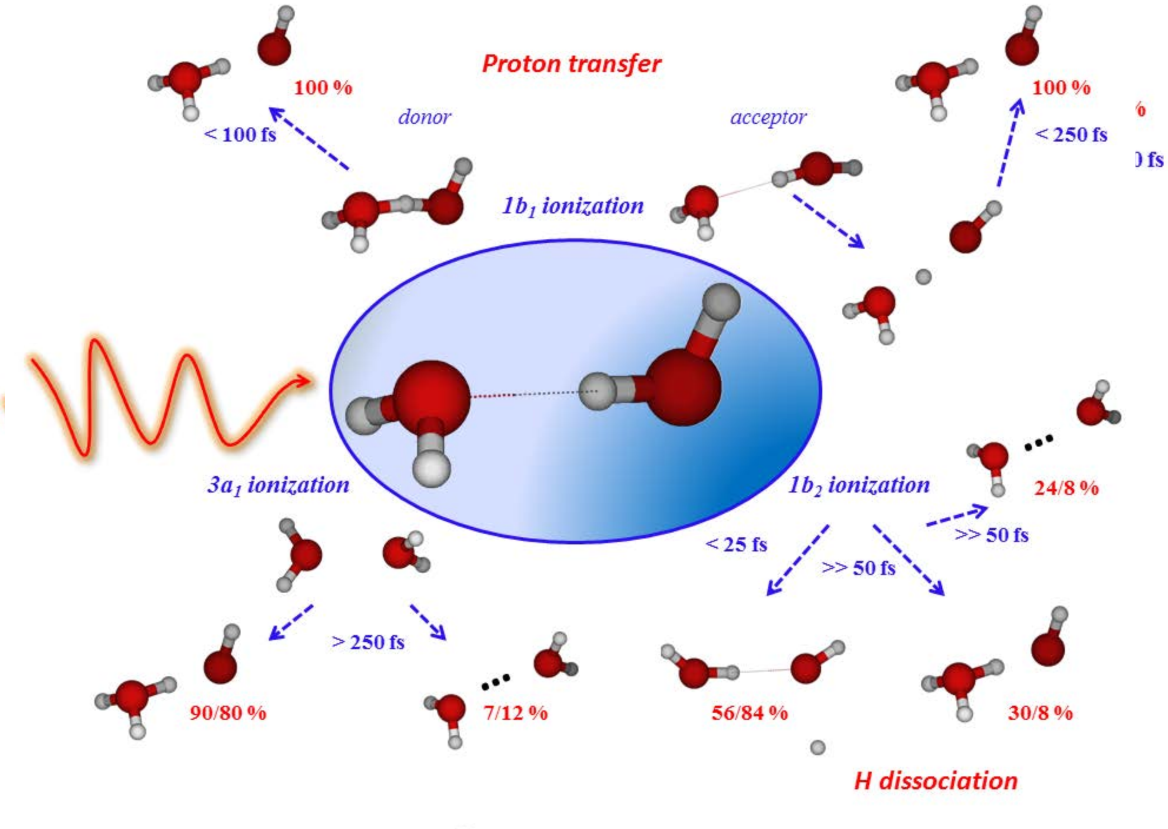

Svoboda, Hollas, Ončák, Slavíček, PhysChemChemPhys. 15 (2013) 11531.

Can We Use Dynamics on the Ground State?

Is internal conversion fast enough?

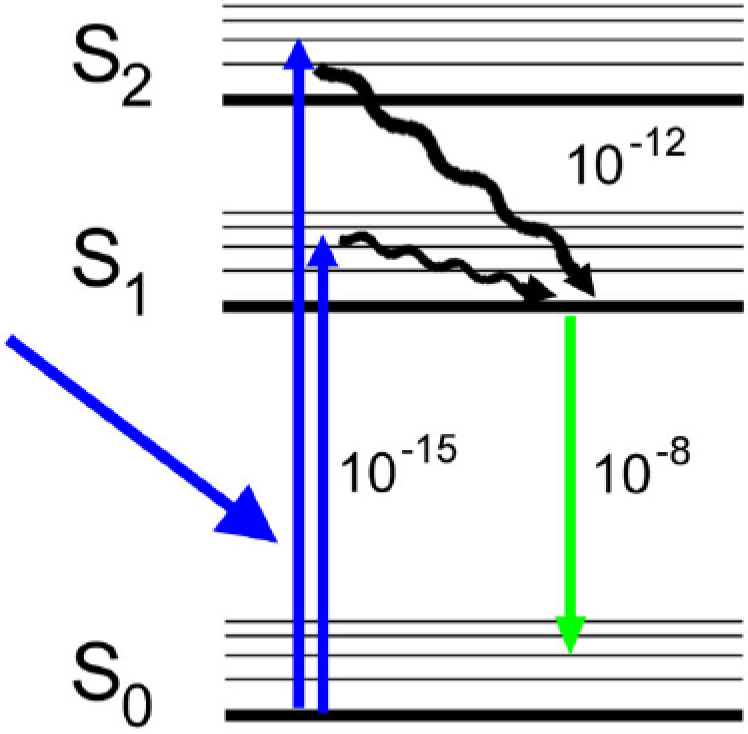

Ammonia dimer

Electronic populations

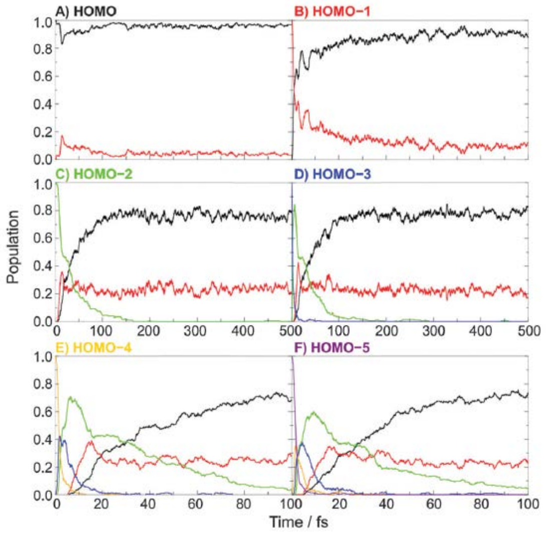

Proton transfer population

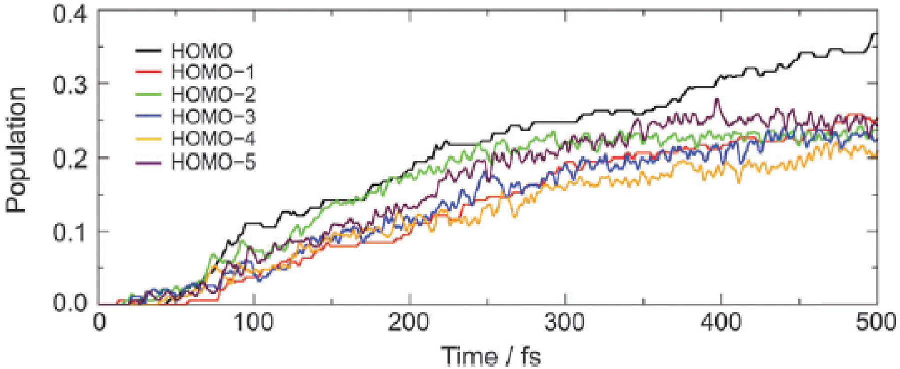

Treating Highly Excited States

Highly excited states are formed within ICD

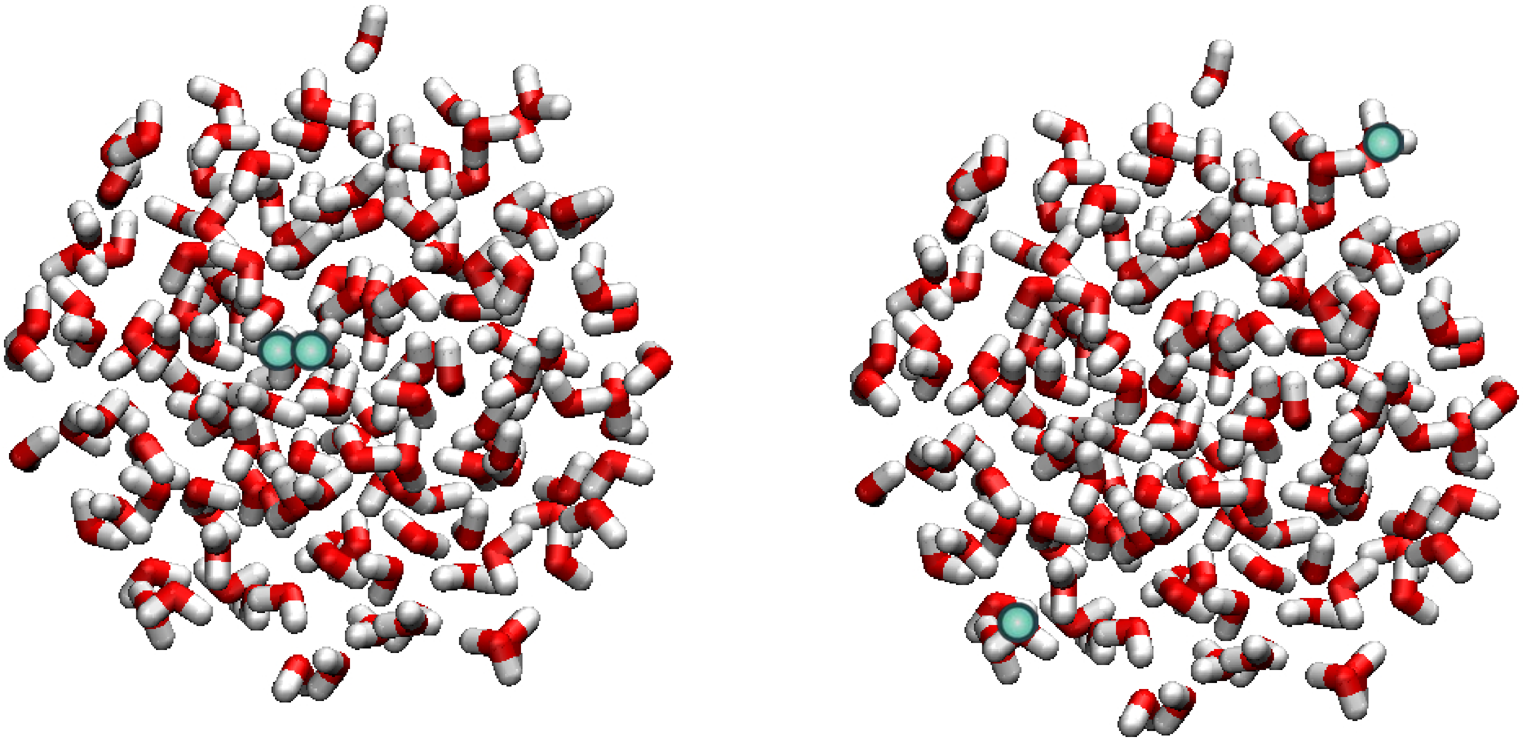

Real time electronic propagation

Electronic Dynamics with TDDFT

Real-time TDDFT: propagating electronic densities

$$i\hbar\frac{\partial\phi_n}{\partial t} = \hat{H}_{KS}\phi_n \qquad \rho(\vec{r},t) = \sum_{n=1}|\phi_n(\vec{r},t)|^2$$

Time-dependent functional

Adiabatic approximation

Coupling with nuclear motion: Ehrenfest dynamics

Involving laser pulse or non-equilibrium initial state

Example: Charge migration in glycine

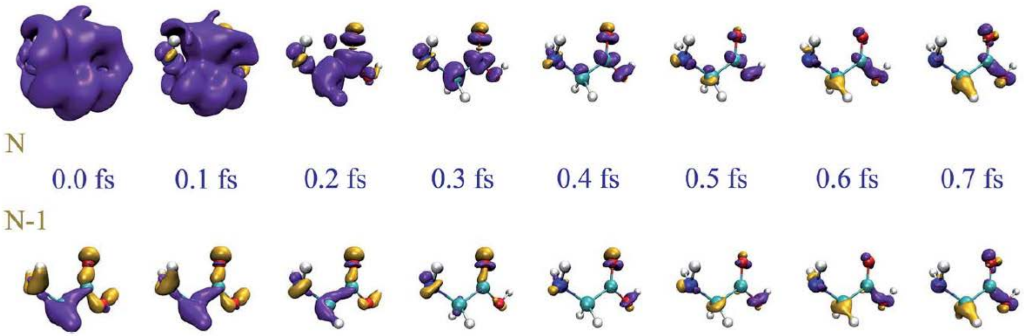

Lara-Astiaso et al., Farad. Disc. 2016, DOI: 10.1039/C6FD00074F

Including Decaying States

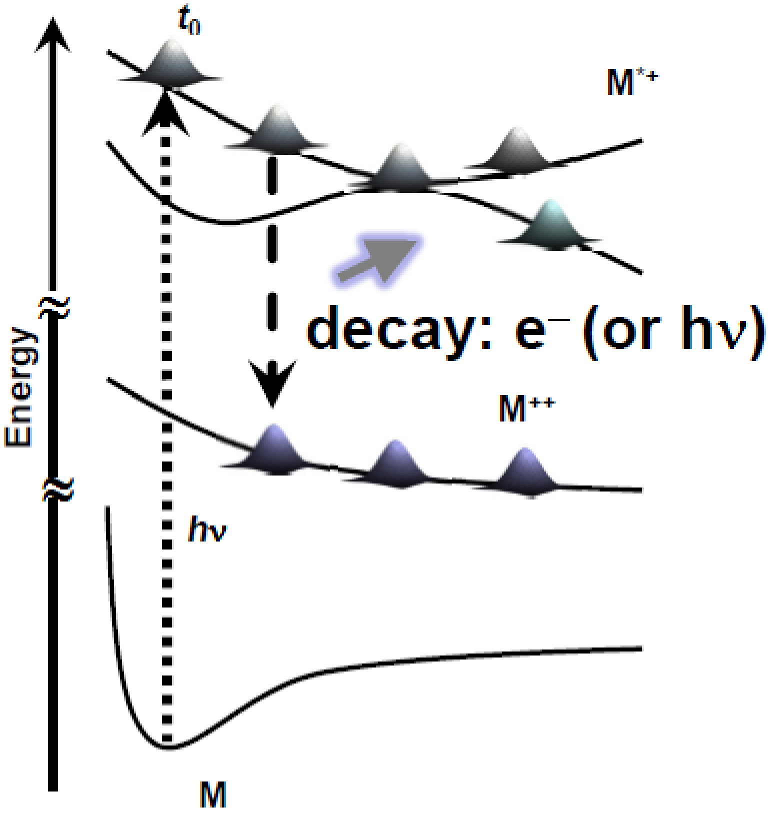

Complex Hamiltonian

$$\hat{H}' = \hat{H} - \frac{i\Gamma}{2}$$

Random hops into the final state

$$A_n(t) = \langle \psi_n(t) | \hat{A} | \psi_n(t) \rangle$$

$$\langle \hat{A} \rangle(t) = \frac{1}{N} \sum_{n=1}^{N} A_n(t)$$

Monte Carlo Wavepackets method

For example: Instantaneous Auger spectrum

$$A_n \equiv \sigma_n^{if} = C^{if} \int |\psi(t_n)|^2 \delta(E_e - V_{fi}) d\vec{R}$$

Including Decaying States

Uncertainity principle

$$L(E) = \frac{1}{\pi} \frac{\frac{\hbar}{2\tau}}{(E - E_{ab})^2 + (\frac{\hbar}{2\tau})^2}$$

Missing Interferences

Auger spectra

$$\sigma(E_e) \sim \Gamma \sum_f \left| \sum_n \frac{\langle f|n\rangle\langle f|n\rangle}{E_e - E_{nf} + i\Gamma} \right|^2$$

(Non-resonant) XES

$$\sigma(E_{ph}) \sim \sum_f \left| \sum_n \frac{\langle f|\vec{\mu}_{FN}|n\rangle\langle n|\vec{\mu}_{NI}|i\rangle}{E_{ph} - E_{nf} + i\Gamma} \right|^2$$

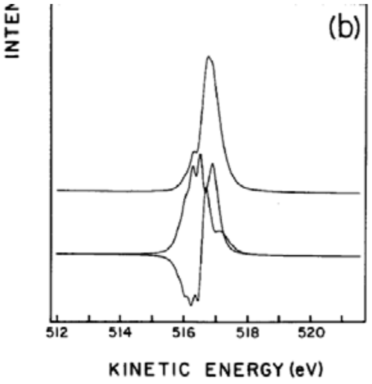

FIG. 2. (a) Computed line shape from Ref. 1 for the oxygen autoionization spectrum of CO. (b) Our computed line shape for this transition using Eq. (1).

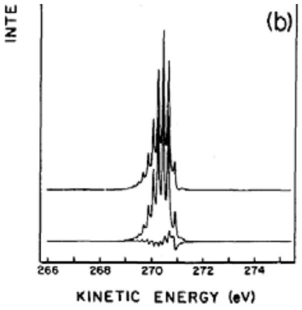

FIG. 1. (a) Computed line shape from Ref. 1 for the carbon autoionization spectrum of CO. (b) Our computed line shape for this transition using Eq. (1) (excited-state and final-state vibrational constants the same as in Ref. 1). In both (a) and (b) the top curve is the full computed spectrum, the middle curve is the "direct" contribution, and the bottom curve is the "interference" curve.

Carrol and Thomas, J. Chem. Phys. 86, 5221 (1987)

Including Decaying States

Classical trajectories with a phase

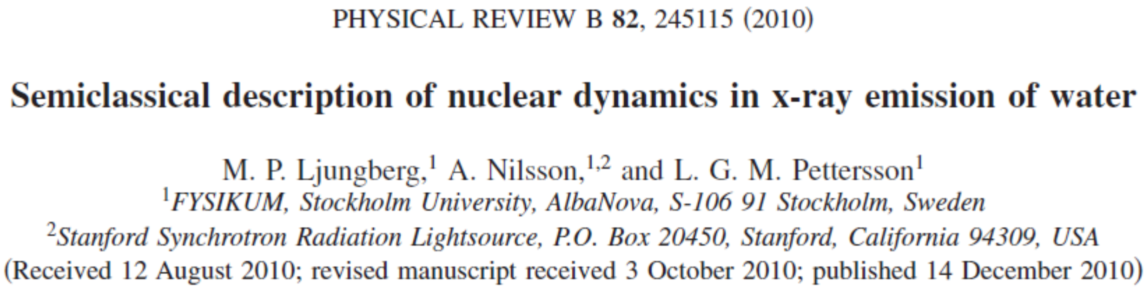
PHYSICAL REVIEW B **82**, 245115 (2010)

Semiclassical description of nuclear dynamics in x-ray emission of water

M. P. Ljungberg,[1] A. Nilsson,[1,2] and L. G. M. Pettersson[1]
[1] *FYSIKUM, Stockholm University, AlbaNova, S-106 91 Stockholm, Sweden*
[2] *Stanford Synchrotron Radiation Lightsource, P.O. Box 20450, Stanford, California 94309, USA*
(Received 12 August 2010; revised manuscript received 3 October 2010; published 14 December 2010)

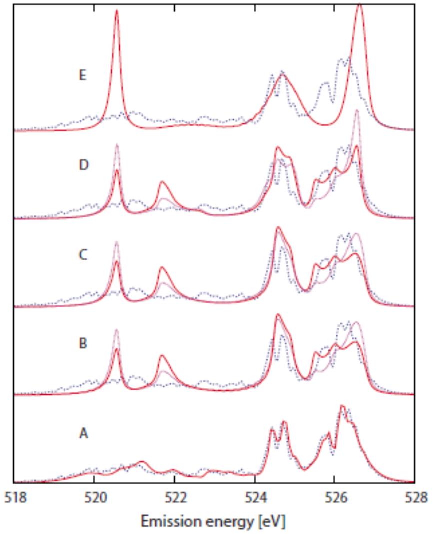

FIG. 3. (Color online) Comparison of the different methods with the full Kramers-Heisenberg formalism (blue, dotted) applied to the H-bonded OH. From bottom to top the full line represents: (a) SCKH with quantum initial conditions sampling both momentum and OH distance distributions, (b) SSWPP, (c) SSCT with quantum initial conditions, (d) SSCT with classical initial conditions, and (e) VA. In (b)–(d) the full line is spectra computed with the longer lifetime and the purple line with closely spaced dots with the shorter one.

$$D_{cl}(E_{ph}) = \int_0^\infty \vec{\mu}_{NI}(0)\vec{\mu}_{FN}(t)e^{-\frac{i}{\hbar}\int_0^t (E_F(\tau)-E_N(\tau))d\tau}\, e^{-i\Gamma t} e^{-\frac{iE_{ph}}{\hbar}t}\, dt$$

$$\sigma(E_{ph}) = \sum_{traj} \left|D_{cl}(E_{ph})\right|^2$$

Coupling to Continuum: Fano Theory

Decaying state

Continuum of final states

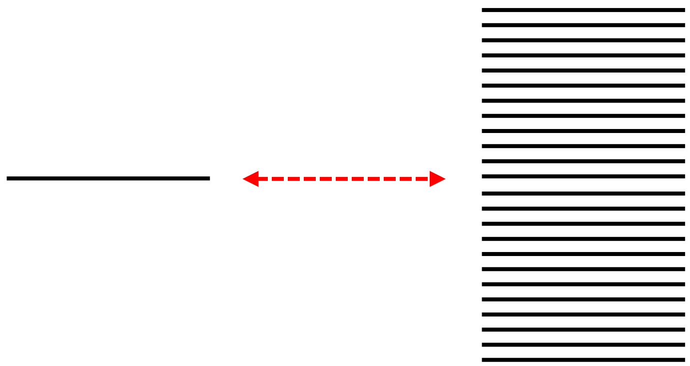

ϕ χ_{E_r}

$|X^{+*}\rangle$ $|X^{++}\rangle$

$$\psi_E = a(E)\phi + \int b(E,\varepsilon)\chi_\varepsilon d\varepsilon$$

$$\hat{H}\psi_E = E\psi_E$$

$$|a(E)|^2 = \frac{\Gamma/2\pi}{(E-E_r)^2 + \Gamma^2/4}$$

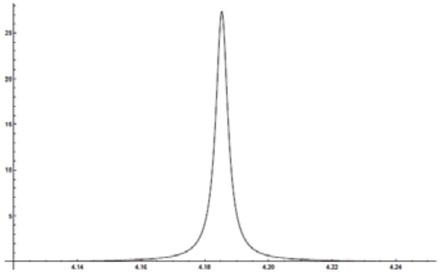

$$\Gamma = 2\pi\left|\langle\phi|\hat{H} - E_r|\chi_{E_r}\rangle\right|^2 \quad \tau = \frac{1}{\Gamma}$$

Fano profile

U. Fano, Effects of Configuration Interaction on Intensities and Phase Shifts, *Phys. Rev.* **124**, 1866-1878 (1961).

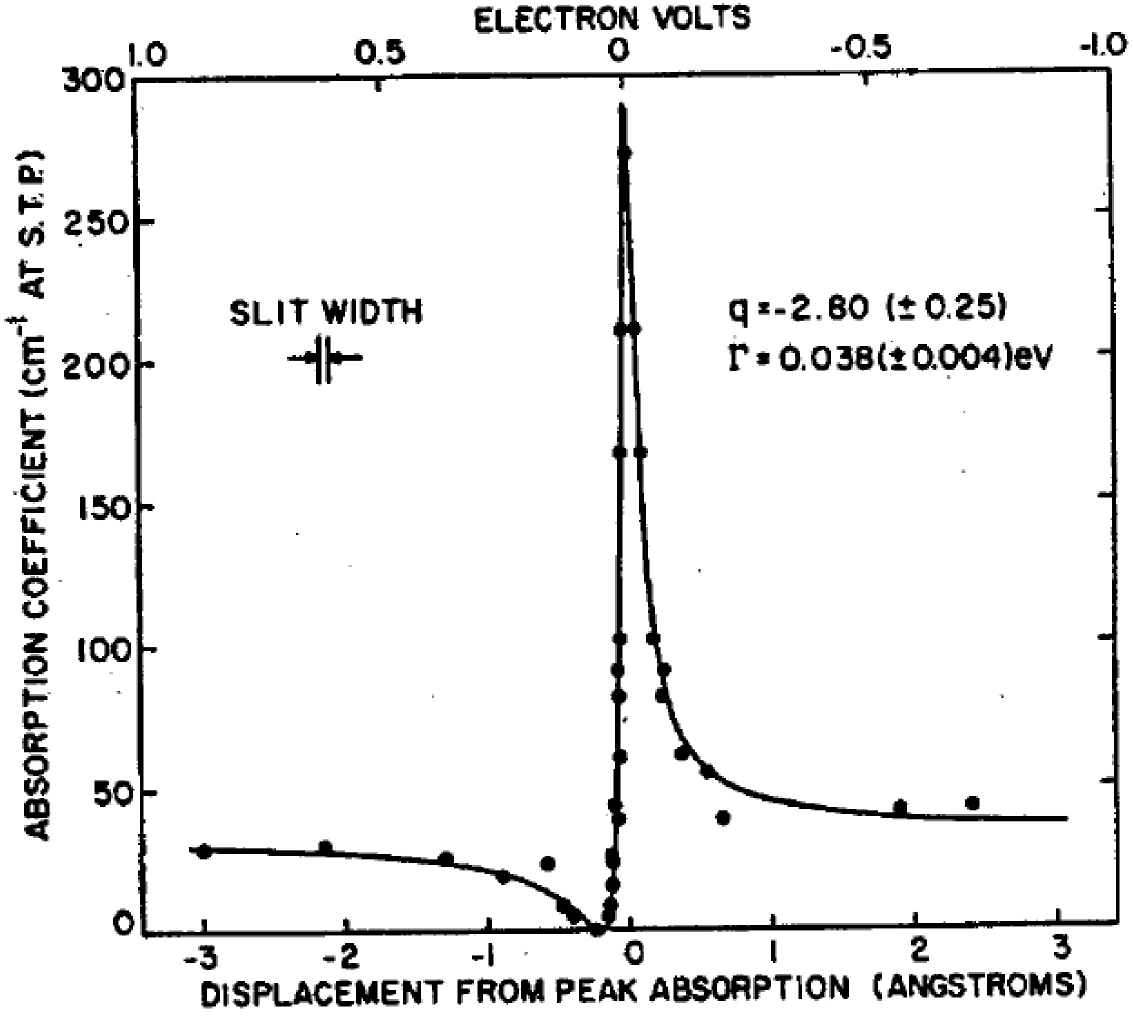

Simplest Case: Hartree-Fock Wavefunction

Initial state $|X^{+*}\rangle$ **represented by a single Slater determinant**

Final state $|X^{++}\rangle$ **represented by N−1 electron function and outgoing electron wave**

Decay width

$$\Gamma = 2\pi \langle X^{+*}|\hat{H}_e|k, X^{++}\rangle \, \delta(E_{X^{+*}} - E_{X^{++}} - E_k) =$$

$$2\pi \sum_k \sum_v \sum_w |V_{v,w[1s,k]}|^2 x$$

$$\delta(\epsilon_{1s} + \epsilon_k - \epsilon_v - \epsilon_w + V_{v,w[v,w]} - V_{k,v[k,w]} - V_{k,w[k,w]})$$

$$V_{v,w[1s,k]} = \int\int \phi_{1s}(\mathbf{r}_1)\phi_k(\mathbf{r}_2)\frac{1}{r_{12}}\phi_v(\mathbf{r}_1)\phi_w(\mathbf{r}_2)\mathrm{d}\mathbf{r}_1\mathrm{d}\mathbf{r}_2$$

Decay Rates With Quantum Chemistry

Technology of quantum chemistry is developed, including excited states

Yet the spectra are (i) discrete (ii) they have wrong normalization

Decay Rates With Quantum Chemistry

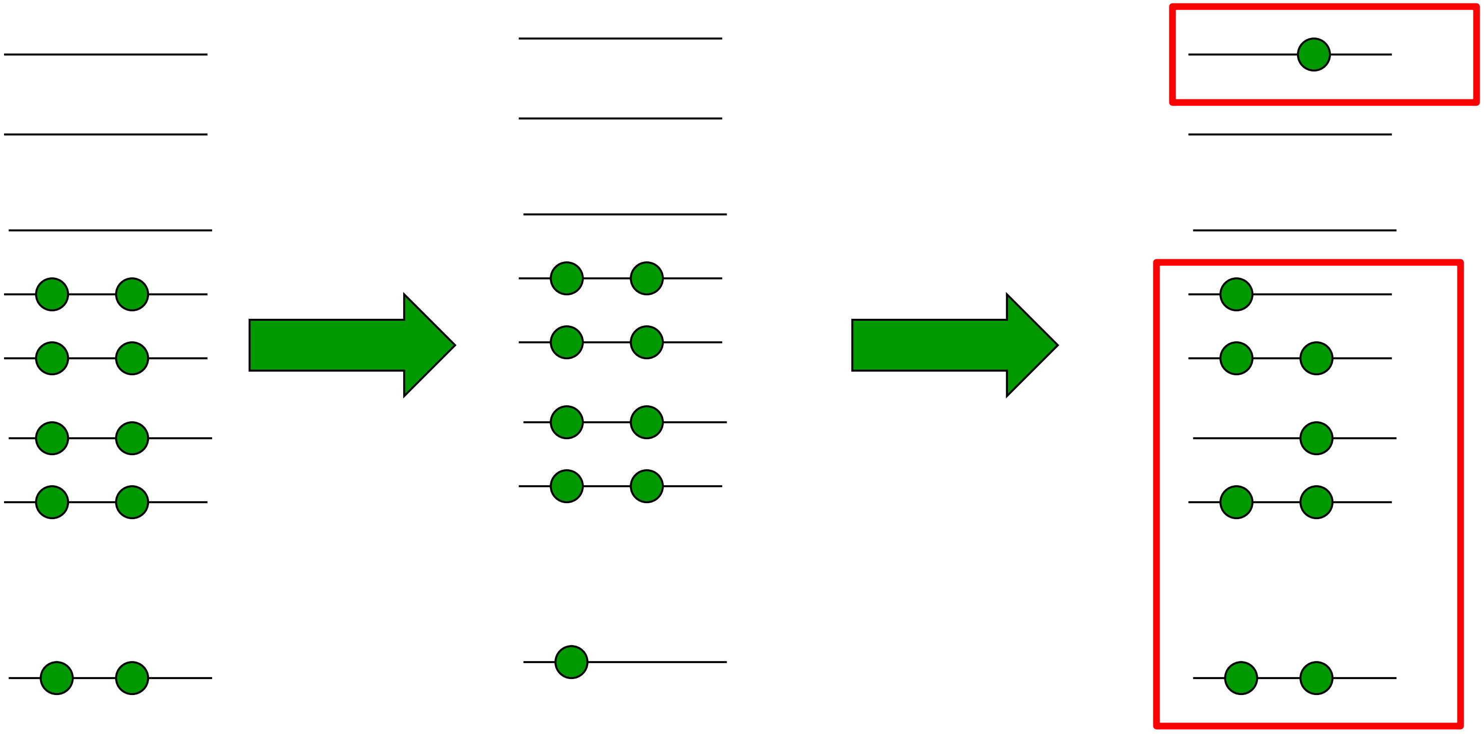

HF neutral state

Initial state

Final state

Decay Rates With Quantum Chemistry

Technology of quantum chemistry is developed, including excited states

Yet the spectra are (i) discrete (ii) they have wrong normalization

Solution: Stieltjes imaging

$$\omega_i \,....\, f_i$$

Analogic procedure for decay widths

$$S(k) = \int_{\omega_T}^{\infty} \omega^k f(\omega) d\omega$$

$$S(k) \approx \sum_{i=1}^{N} \bar{\omega}_i^k \bar{f}_i$$

Non-Hermitian Quantum Chemistry

Quantum chemistry with complex absorbing potential

Imaginary potential is placed on the boundaries of the system

$$\hat{H}(\eta) = \hat{H} - i\eta W$$

Extrapolation to zero CAP

$$E = \lim_{\eta \to 0} E(\eta)$$

The energies of metastable state are complex

$$E = E_R - i\frac{\Gamma}{2}$$

$$\psi(\vec{r}, t) = e^{-iEt}\phi_R(\vec{r}) = e^{-\frac{\Gamma}{2}t}e^{-iE_R t}\phi_R(\vec{r})$$

Autoionization within RT-TDDFT

Overcoming exponential bottleneck with DFT

Can TDDFT describe properly auto-ionization?

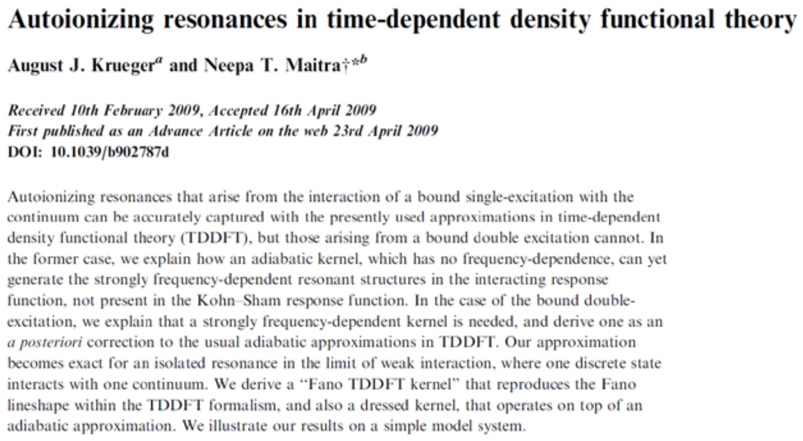

Autoionizing resonances in time-dependent density functional theory

August J. Krueger[a] and Neepa T. Maitra†*[b]

Received 10th February 2009, Accepted 16th April 2009
First published as an Advance Article on the web 23rd April 2009
DOI: 10.1039/b902787d

Autoionizing resonances that arise from the interaction of a bound single-excitation with the continuum can be accurately captured with the presently used approximations in time-dependent density functional theory (TDDFT), but those arising from a bound double excitation cannot. In the former case, we explain how an adiabatic kernel, which has no frequency-dependence, can yet generate the strongly frequency-dependent resonant structures in the interacting response function, not present in the Kohn–Sham response function. In the case of the bound double-excitation, we explain that a strongly frequency-dependent kernel is needed, and derive one as an *a posteriori* correction to the usual adiabatic approximations in TDDFT. Our approximation becomes exact for an isolated resonance in the limit of weak interaction, where one discrete state interacts with one continuum. We derive a "Fano TDDFT kernel" that reproduces the Fano lineshape within the TDDFT formalism, and also a dressed kernel, that operates on top of an adiabatic approximation. We illustrate our results on a simple model system.

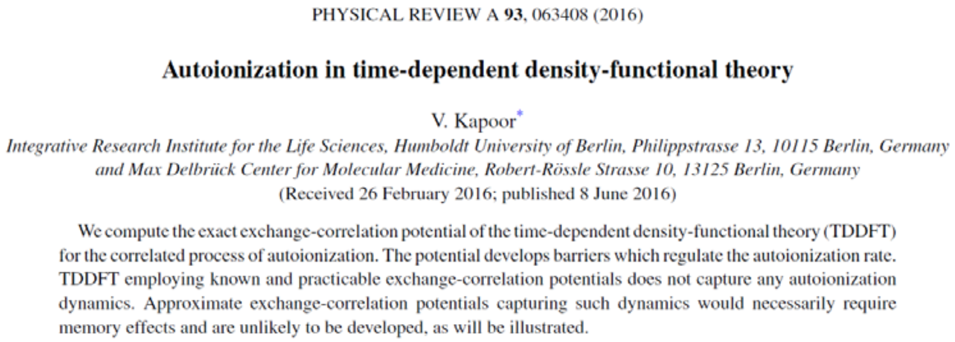

PHYSICAL REVIEW A **93**, 063408 (2016)

Autoionization in time-dependent density-functional theory

V. Kapoor*
Integrative Research Institute for the Life Sciences, Humboldt University of Berlin, Philippstrasse 13, 10115 Berlin, Germany and Max Delbrück Center for Molecular Medicine, Robert-Rössle Strasse 10, 13125 Berlin, Germany
(Received 26 February 2016; published 8 June 2016)

We compute the exact exchange-correlation potential of the time-dependent density-functional theory (TDDFT) for the correlated process of autoionization. The potential develops barriers which regulate the autoionization rate. TDDFT employing known and practicable exchange-correlation potentials does not capture any autoionization dynamics. Approximate exchange-correlation potentials capturing such dynamics would necessarily require memory effects and are unlikely to be developed, as will be illustrated.

Problem: Adiabatic approximation

Thrifty Estimate of the Lifetime: Population Analysis

Auger decay is dominated by on-site processes

$$V_{v,w[1s,k]} = \int\int \phi_{1s}(\mathbf{r}_1)\phi_k(\mathbf{r}_2)\frac{1}{r_{12}}\phi_v(\mathbf{r}_1)\phi_w(\mathbf{r}_2)\mathrm{d}\mathbf{r}_1\mathrm{d}\mathbf{r}_2$$

Cooking the Auger intensities based on the atomic contributions

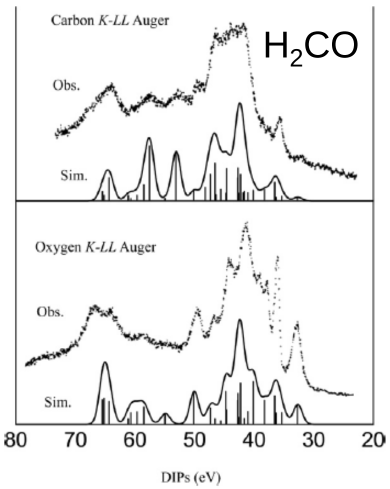

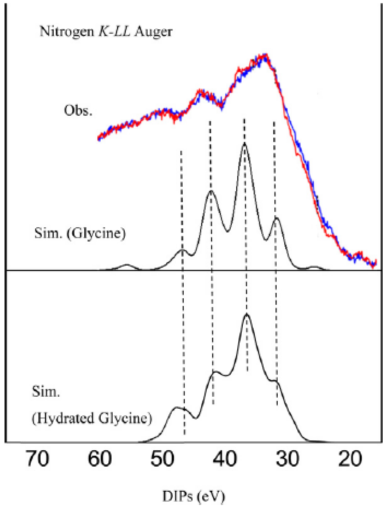

Relative importance of different channels

“Core hole clock”

Y. Hori et al. / Journal of Electron Spectroscopy and Related Phenomena 207 (2016) 60–64

Electronic Force Field Approach

Su and Goddard: “Classical” electron

$$\Psi(\mathbf{r}) \propto \prod_i \exp\left[-\left(\frac{1}{s_i^2} - \frac{2p_{s,i}}{s_i} i\right)(\mathbf{r}-\mathbf{x_i})^2\right] \cdot \exp[i\mathbf{p_{x,i}} \cdot \mathbf{r}]$$

$$E = E_{\text{ke}} + E_{\text{nuc·nuc}} + E_{\text{nuc·elec}} + E_{\text{elec·elec}} + E_{\text{Pauli}}$$

$$E_{\text{ke}} = \sum_i \frac{3}{2}\frac{1}{s_i^2} \qquad E_{\text{nuc·nuc}} = \sum_{i<i} \frac{Z_i Z_j}{R_{ij}} \qquad E_{\text{nuc·elec}} = -\sum_{i,j} \frac{Z_i}{R_{ij}} \text{Erf}\left(\frac{\sqrt{2}R_{ij}}{s_i}\right)$$

$$E_{\text{elec·elec}} = \sum_{i<j} \frac{1}{x_{ij}} \text{Erf}\left(\frac{\sqrt{2}x_{ij}}{\sqrt{s_i^2 + s_j^2}}\right) \qquad E_{\text{Pauli}} = \sum_{\sigma_i=\sigma_j} E(\uparrow\uparrow)_{ij} + \sum_{\sigma_i\neq\sigma_j} E(\uparrow\downarrow)_{ij}$$

Modelling Auger processes

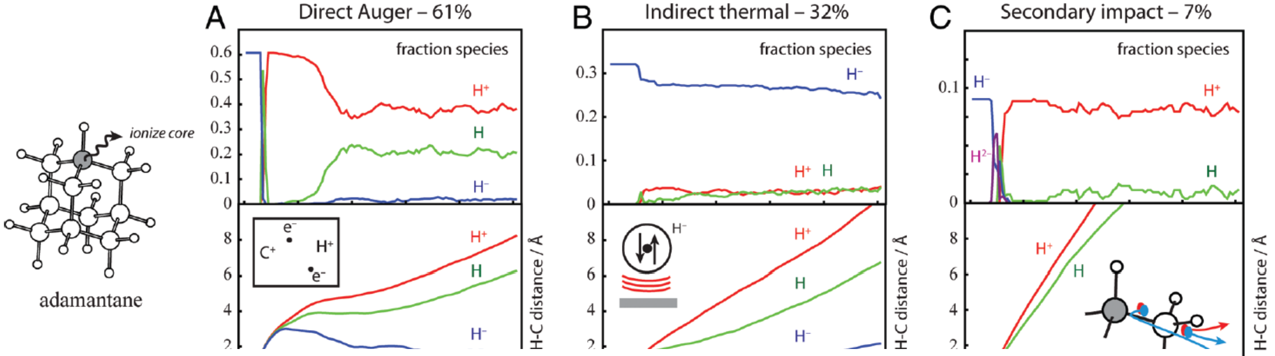

PNAS | January 27, 2009 | vol. 106 | no. 4 | 1001–1005

Spectroscopy Signatures of Nuclear Motion

X-ray photoemission: Water and ice

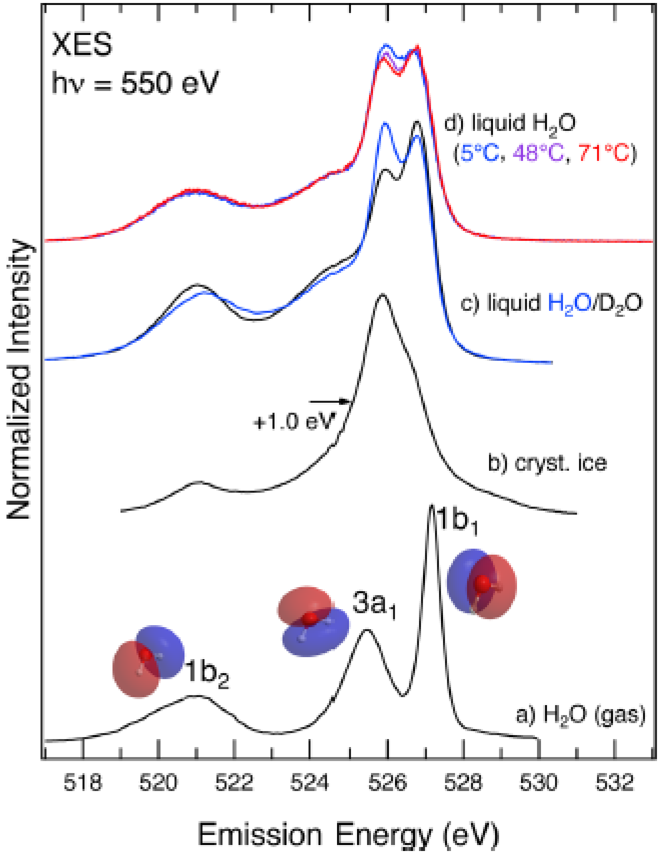

Figure 10. Nonresonantly excited XES spectra of (a) H_2O in the gas phase. Reproduced with permission from ref 136. Copyright 2012 AIP Publishing LLC. (b) Crystalline ice. Reproduced with permission from ref 137. Copyright 1982 AIP Publishing LLC. (c) Liquid H_2O and D_2O at 7 °C. Reproduced with permission from ref 46. Copyright 2008 American Physical Society. (d) Liquid H_2O for three different temperatures. Reproduced with permission from ref 46. Copyright 2008 American Physical Society.

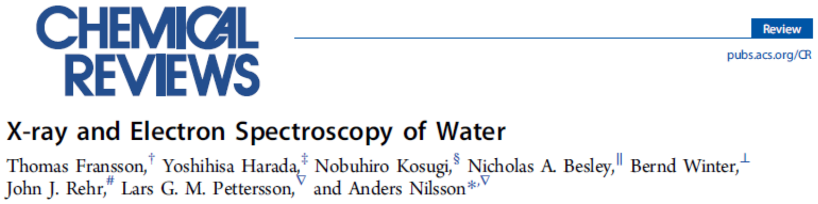

CHEMICAL REVIEWS

Review

pubs.acs.org/CR

X-ray and Electron Spectroscopy of Water

Thomas Fransson,[†] Yoshihisa Harada,[‡] Nobuhiro Kosugi,[§] Nicholas A. Besley,[∥] Bernd Winter,[⊥] John J. Rehr,[#] Lars G. M. Pettersson,[∇] and Anders Nilsson[*,∇]

Auger Spectra of Liquid Water

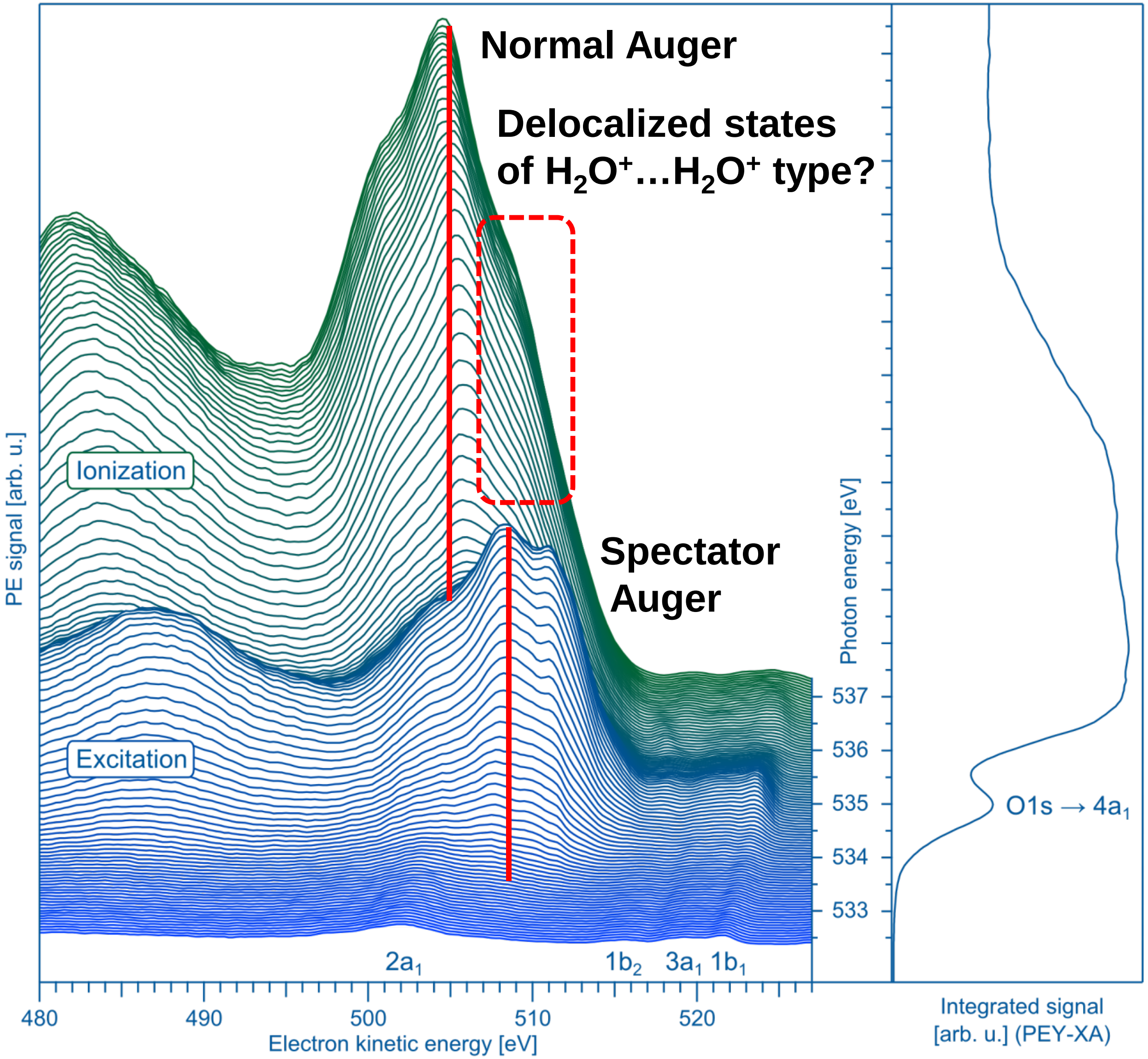

Normal Auger

Delocalized states of $H_2O^+ \ldots H_2O^+$ type?

Spectator Auger

Bernd Winter, BESSY Berlin

Auger Spectra of Liquid Water: Solvent Effects

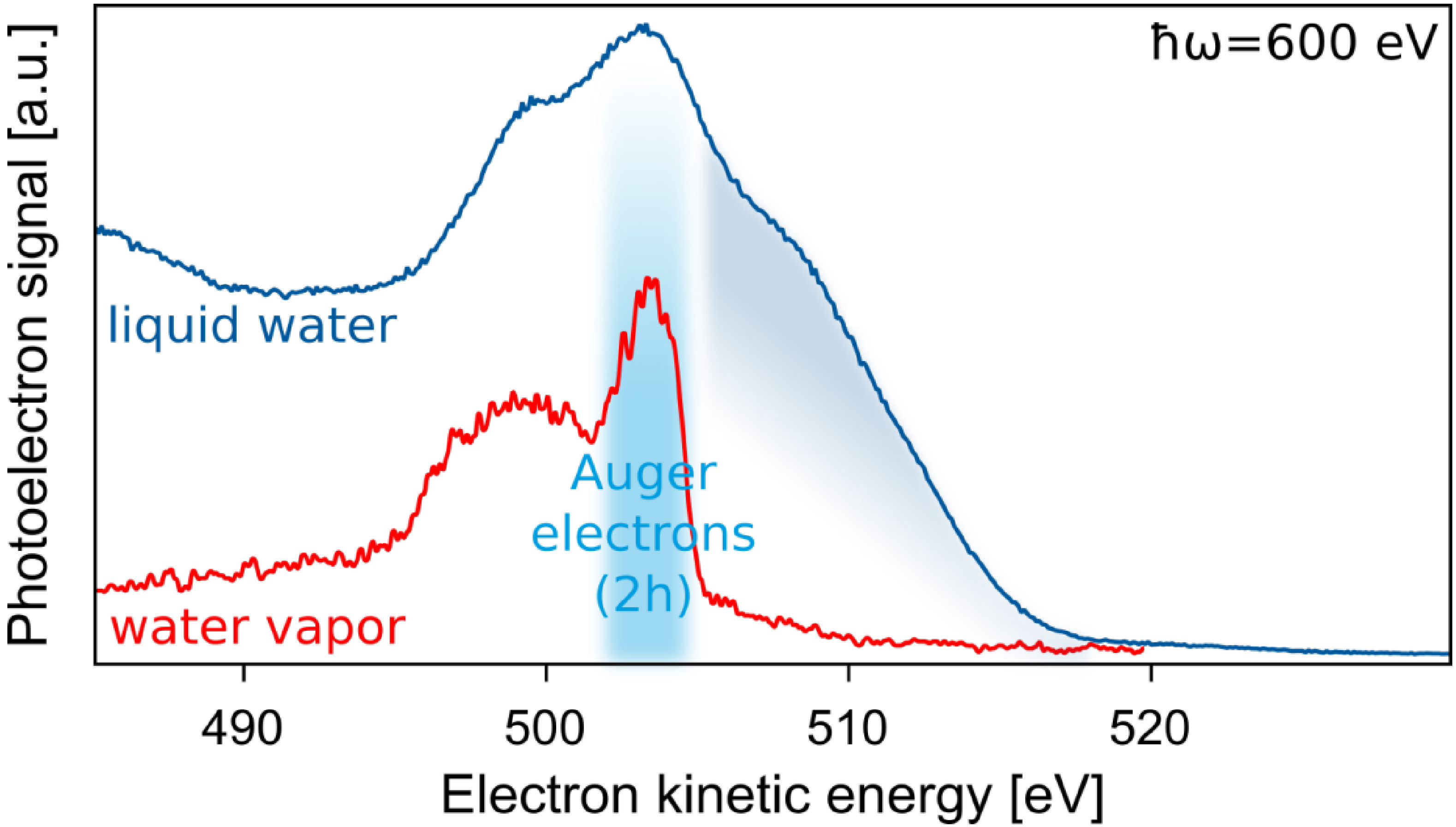

Auger Spectra of Liquid Water: Isotope Effects

Photoelectrons

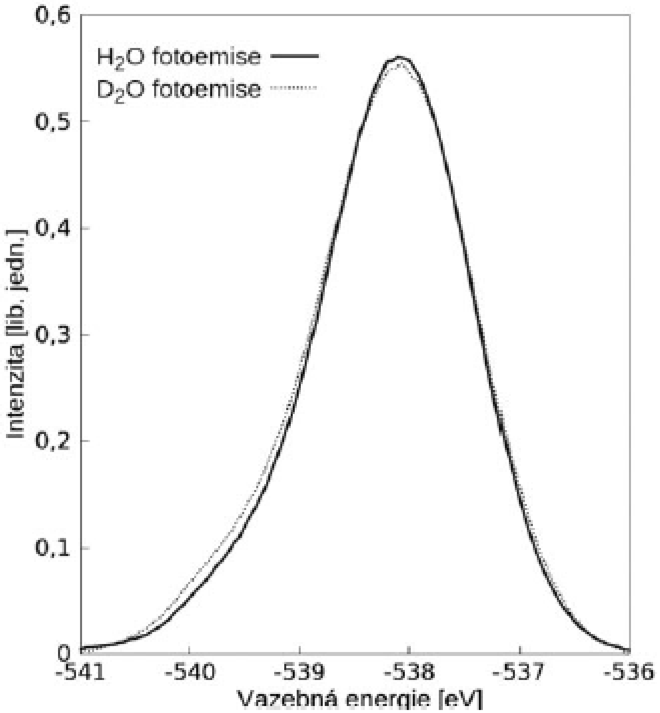

Auger electrons

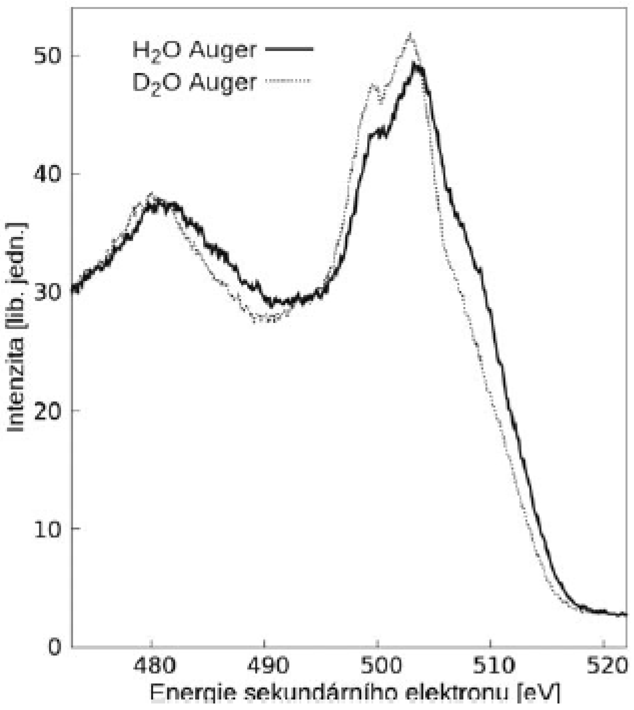

Auger Spectra of Liquid Water

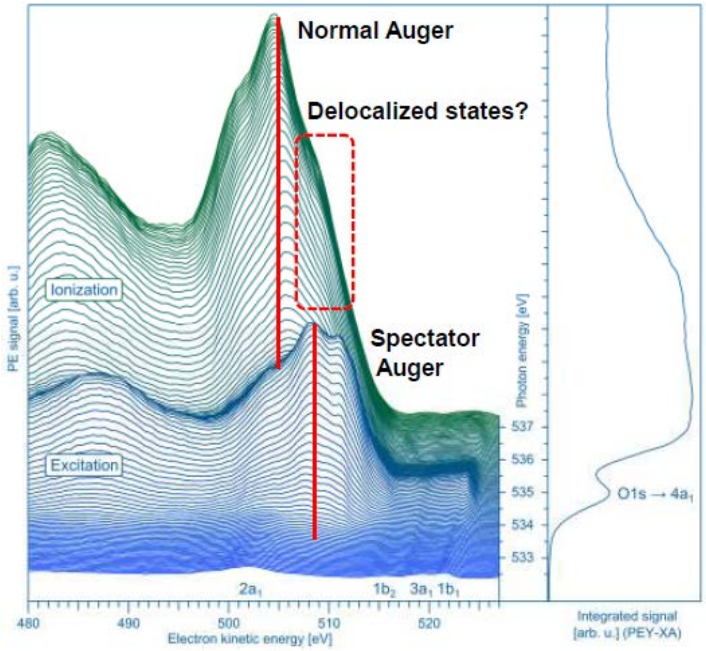

Bernd Winter, BESSY Berlin

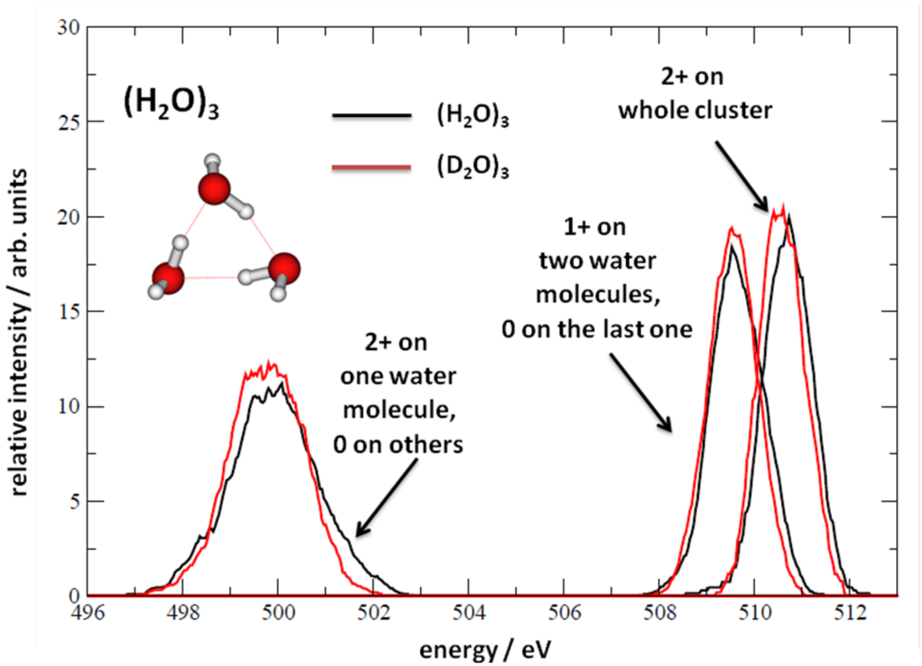

CDFT calculations

Strong isotope dependence of the fast electron peak

Electron and Nuclear Dynamics in Water

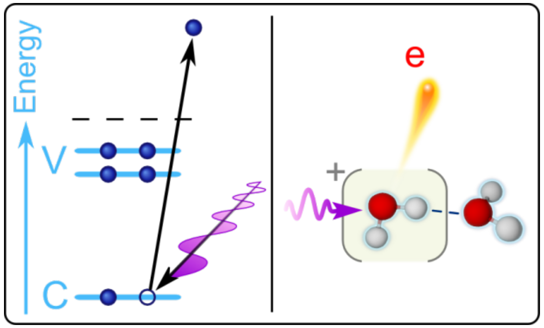

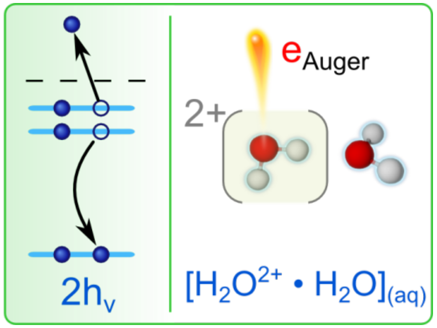

Normal Auger

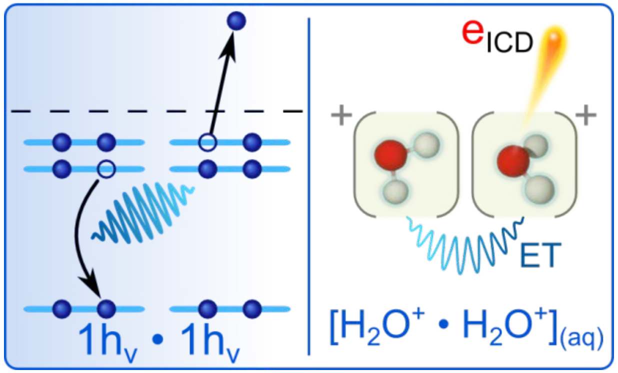

Intermolecular Coulomb Decay (ICD)

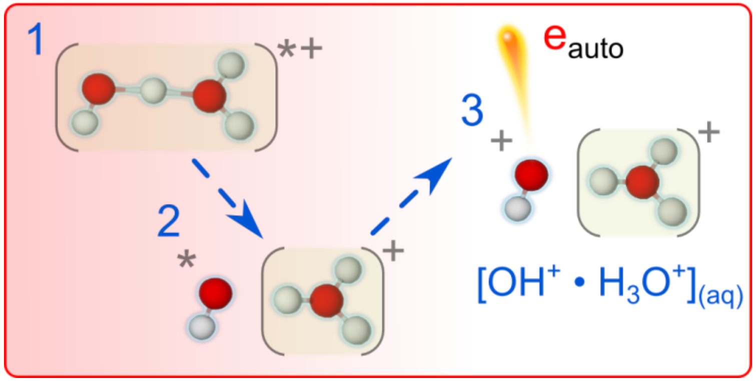

Proton Transfer Mediated Charge Transfer (PTM-CS)

Thürmer, Ončák, Ottosson, Seidel, Hergenhahn, Bradforth, Slavíček, Winter, Nat. Chemistry 5 (2013) 590.

Ultrafast Proton Transfer on Core Ionized State

Flat PES of core ionized state

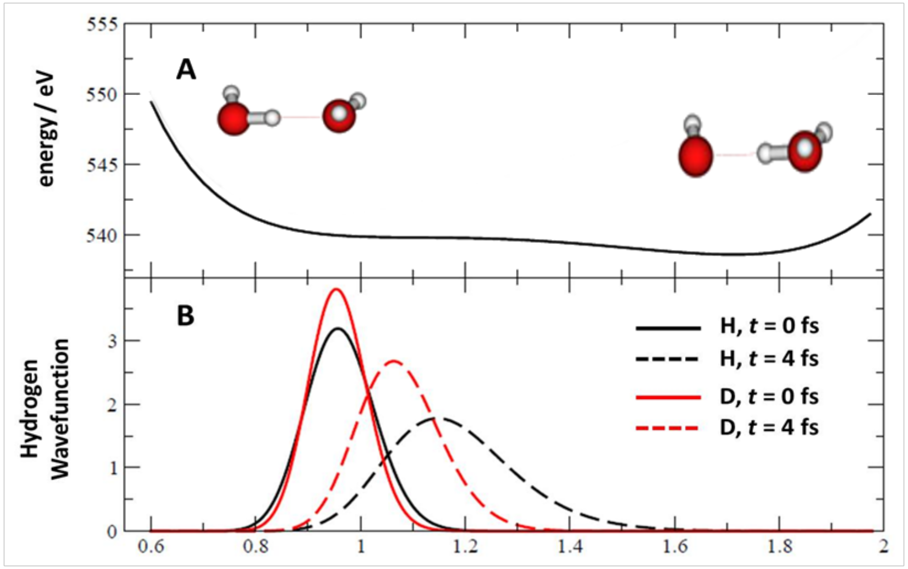

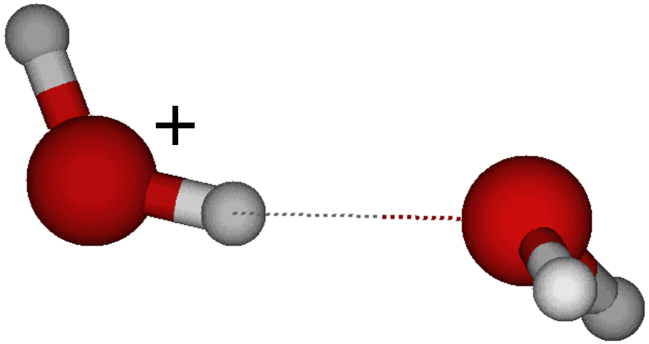

Dispersion of the wavepacket

$$x(t) = x_0 + \frac{p_0}{m}(t - t_0) + \frac{F_0}{m}(t - t_0)^2 \ldots$$

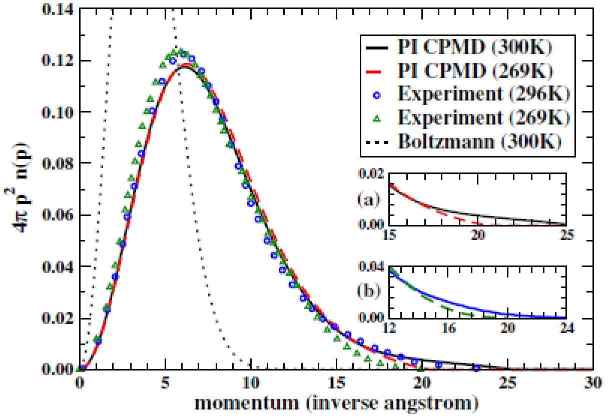

FIG. 3 (color online). The radial proton momentum distribution is reported in the liquid (solid line) and solid (dashed line) phases and plotted against the experimental liquid (circles) and solid (triangles) curves [2], as well as the Boltzmann distribution (dashed line) at 300 K. The insets (a) and (b) depict the tail of the liquid (solid line) and solid (dashed line) distributions, in the simulation and experiment, respectively.

Morrone, Car PRL 101 (2008) 017801

Calculated Auger Spectrum

Experiment

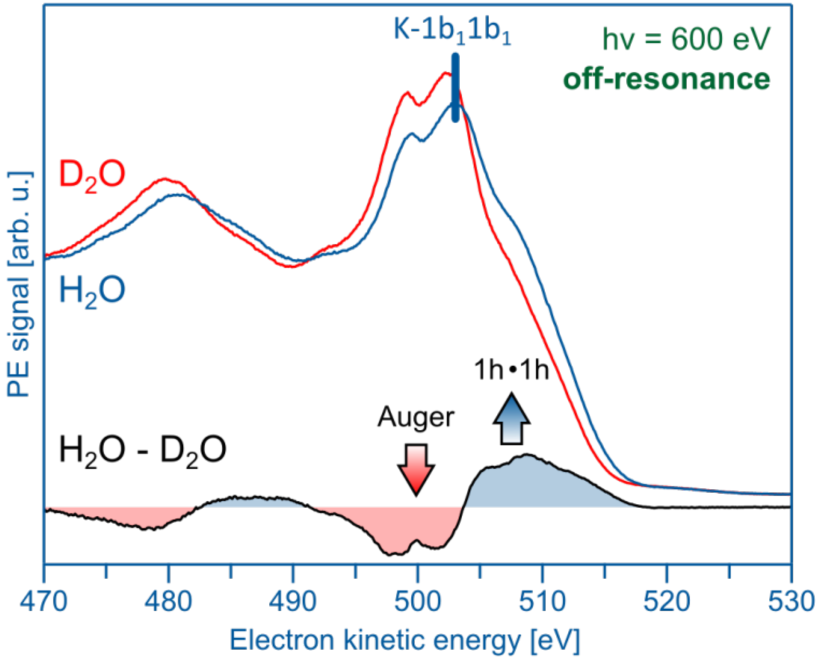

Calculations

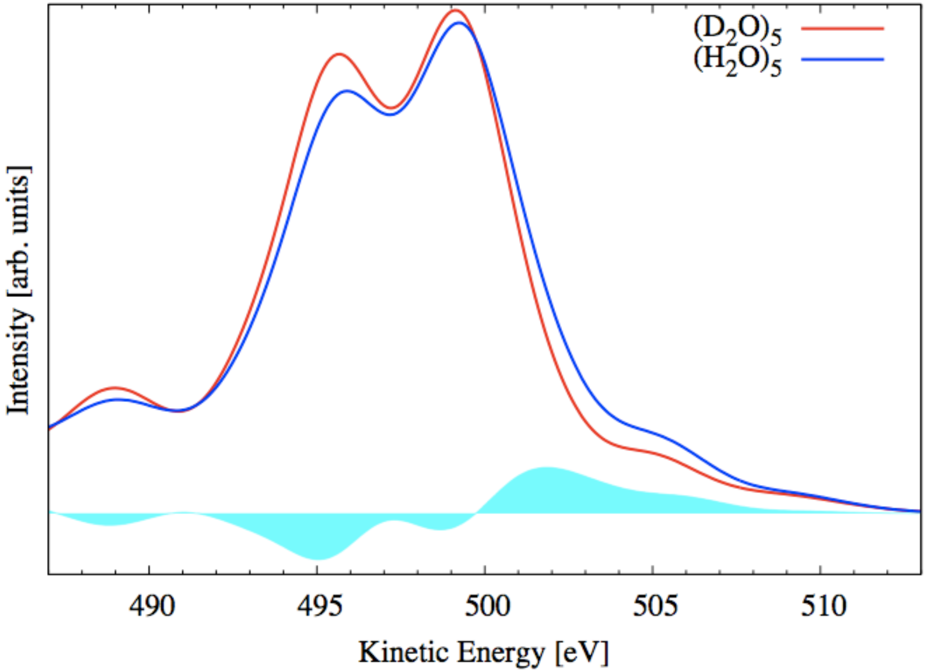

Slavíček, Winter, Cederbaum, Kryzhevoi, JACS, 136 (2014) 18170.

Entangled Electron and Nuclear Dynamics

Relaxation processes at different snapshots

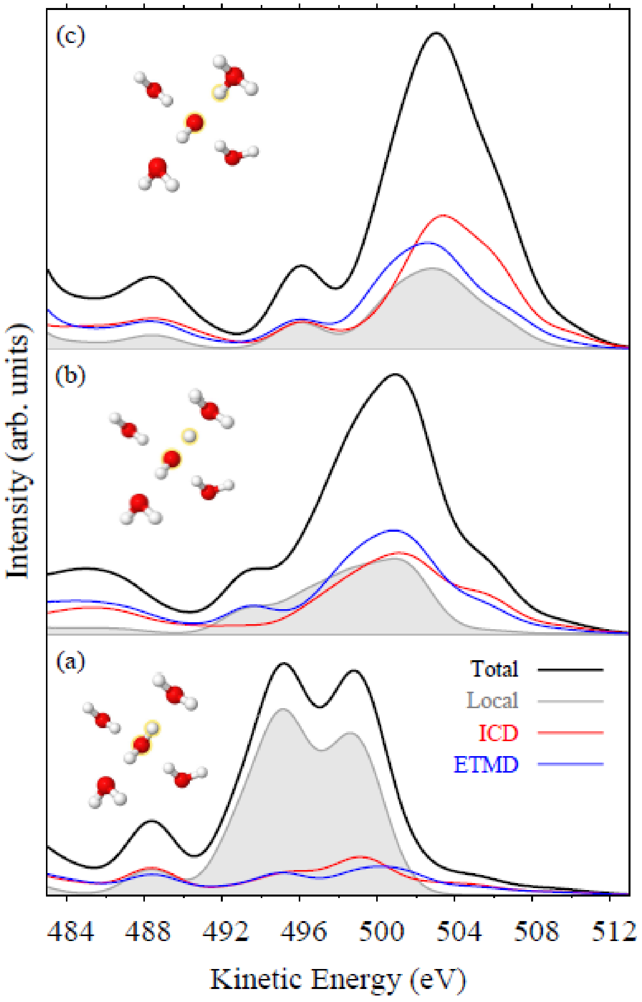

Time evolution

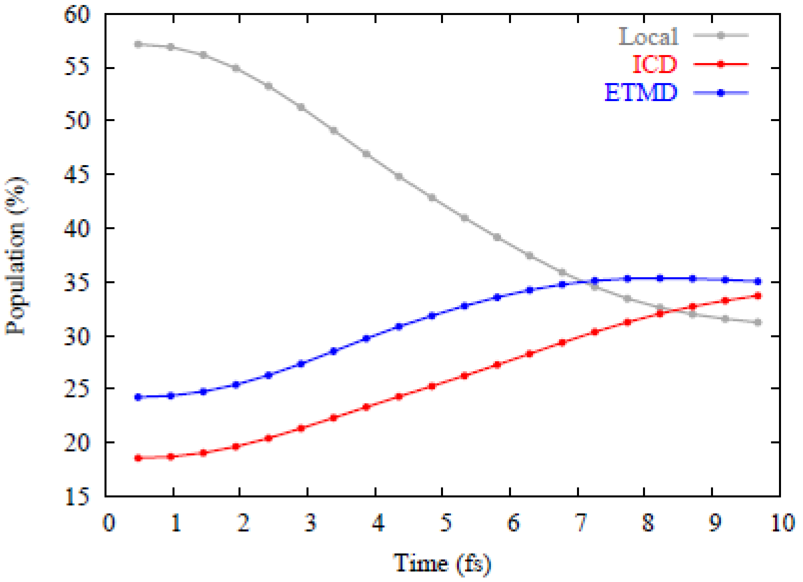

Various final states

Auger: H_2O^{2+}

PTM-Auger: $H_3O^+ \dots OH^+$

ICD, PTM-ICD: $H_2O^{\bullet+} \dots H_2O^{\bullet+}$

Slavíček, Winter, Cederbaum, Kryzhevoi, JACS, 136 (2014) 18170.

Entangled Electron and Nuclear Dynamics

Ammonium cation…

…with double proton transfer

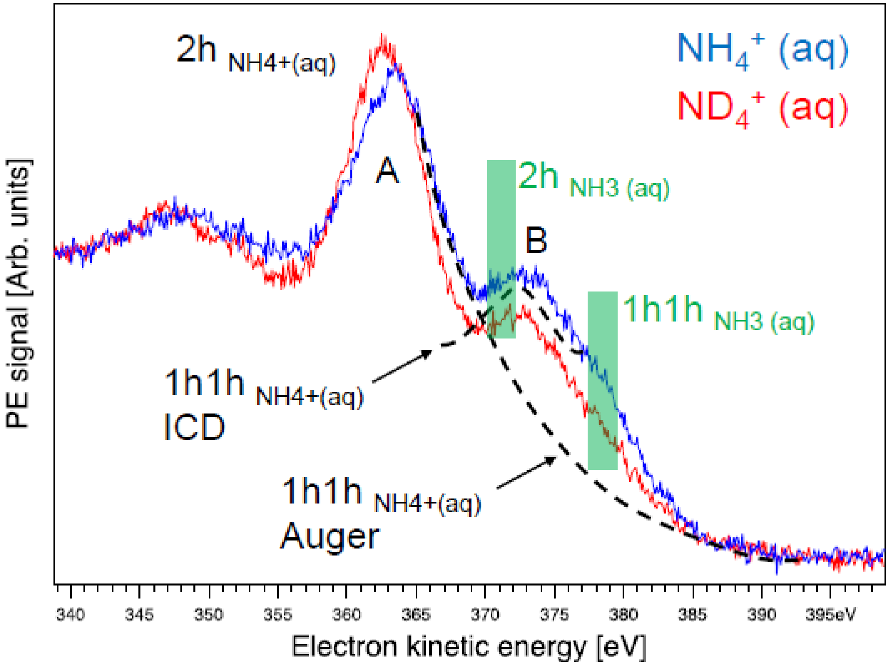

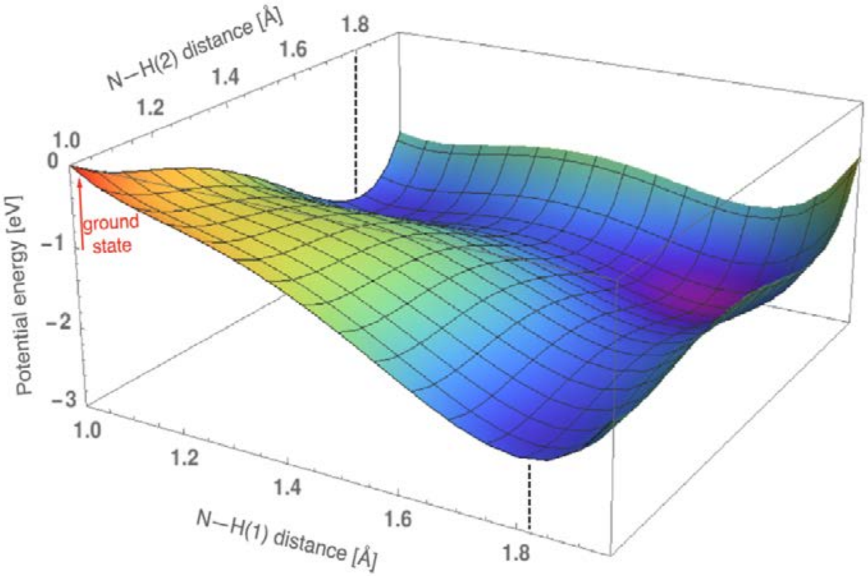

Entangled Electron and Nuclear Dynamics

Double proton transfer observed

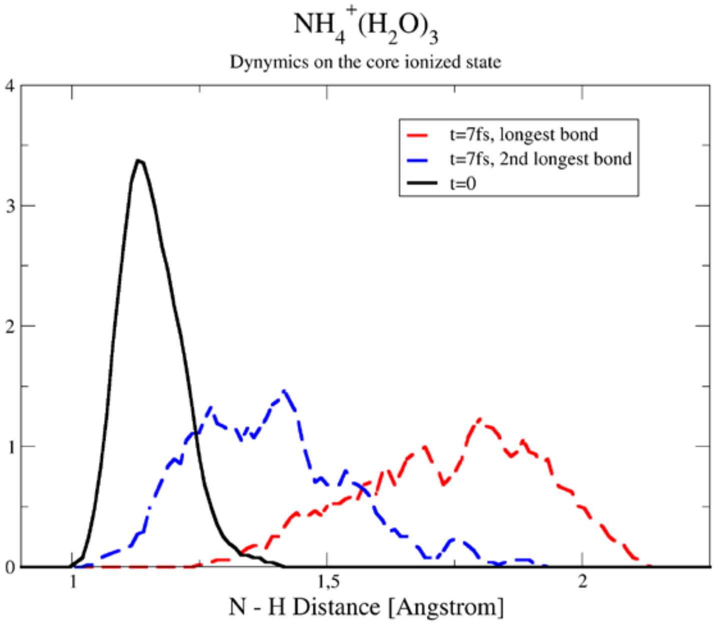
$NH_4^+(H_2O)_3$

Dynymics on the core ionized state

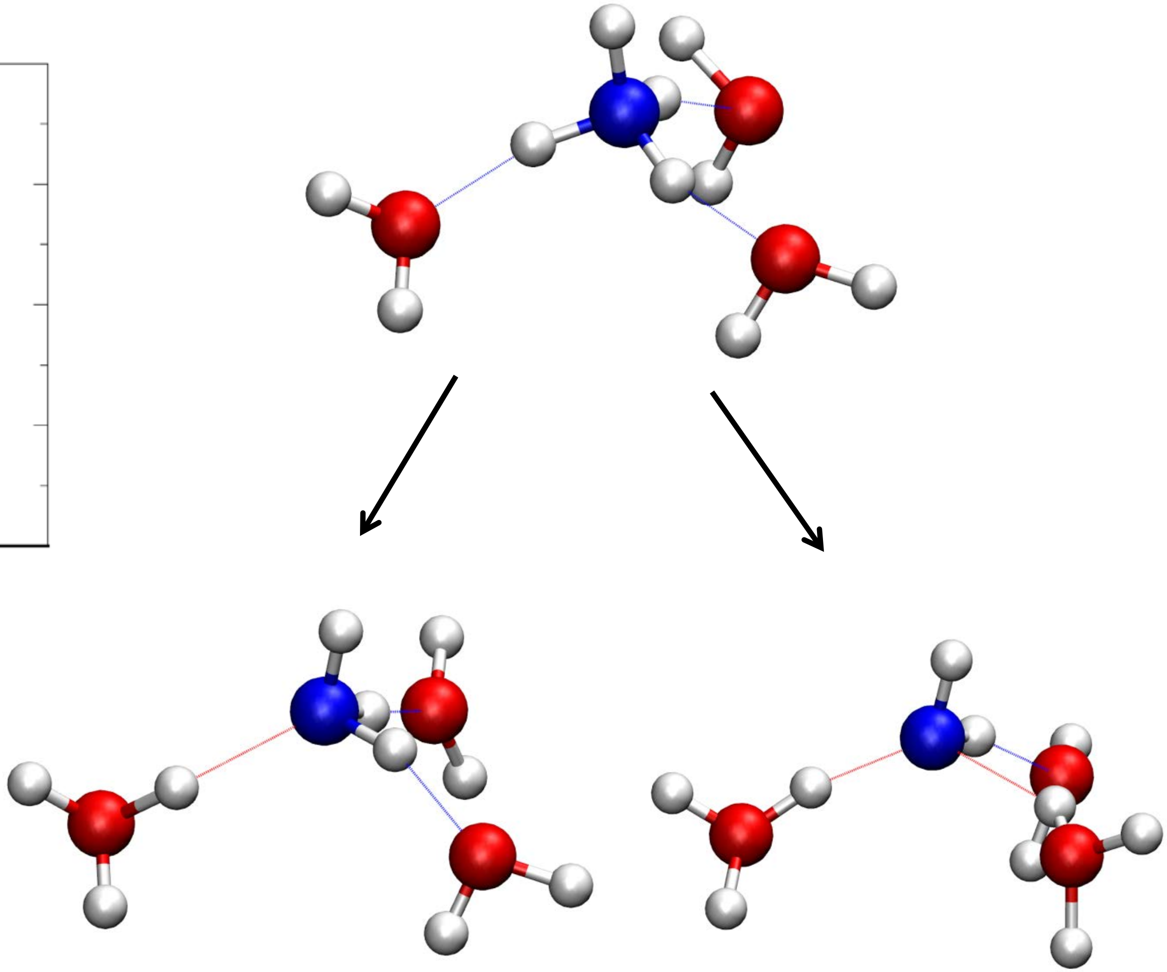

Liquid Structure via PTM-CS

Probing strength of hydrogen bond

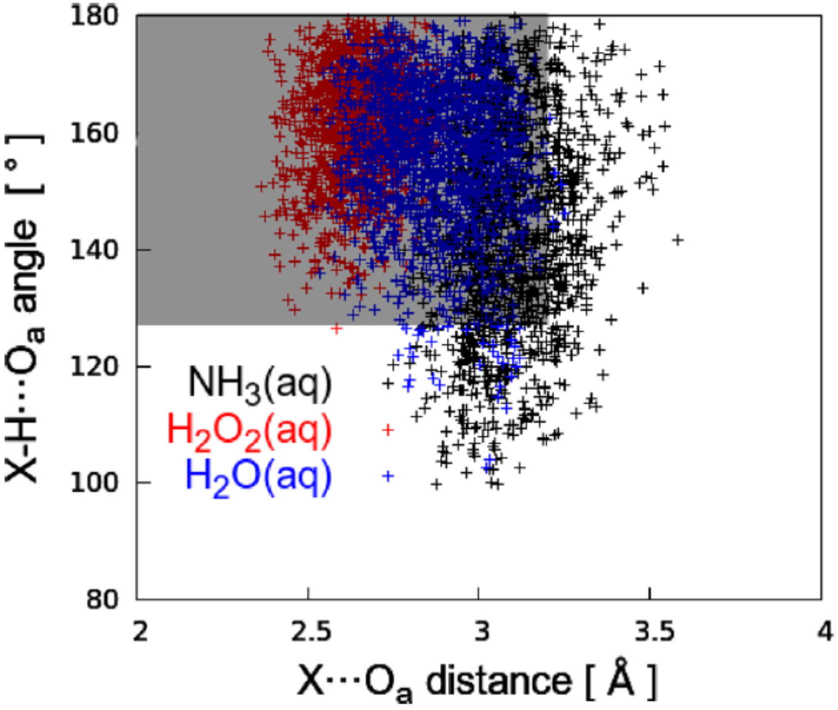

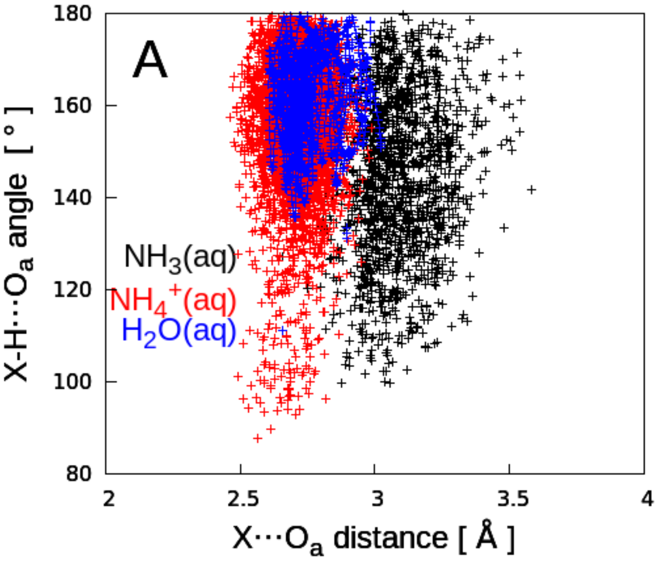

Closing and Opening ICD by Nuclear Motion

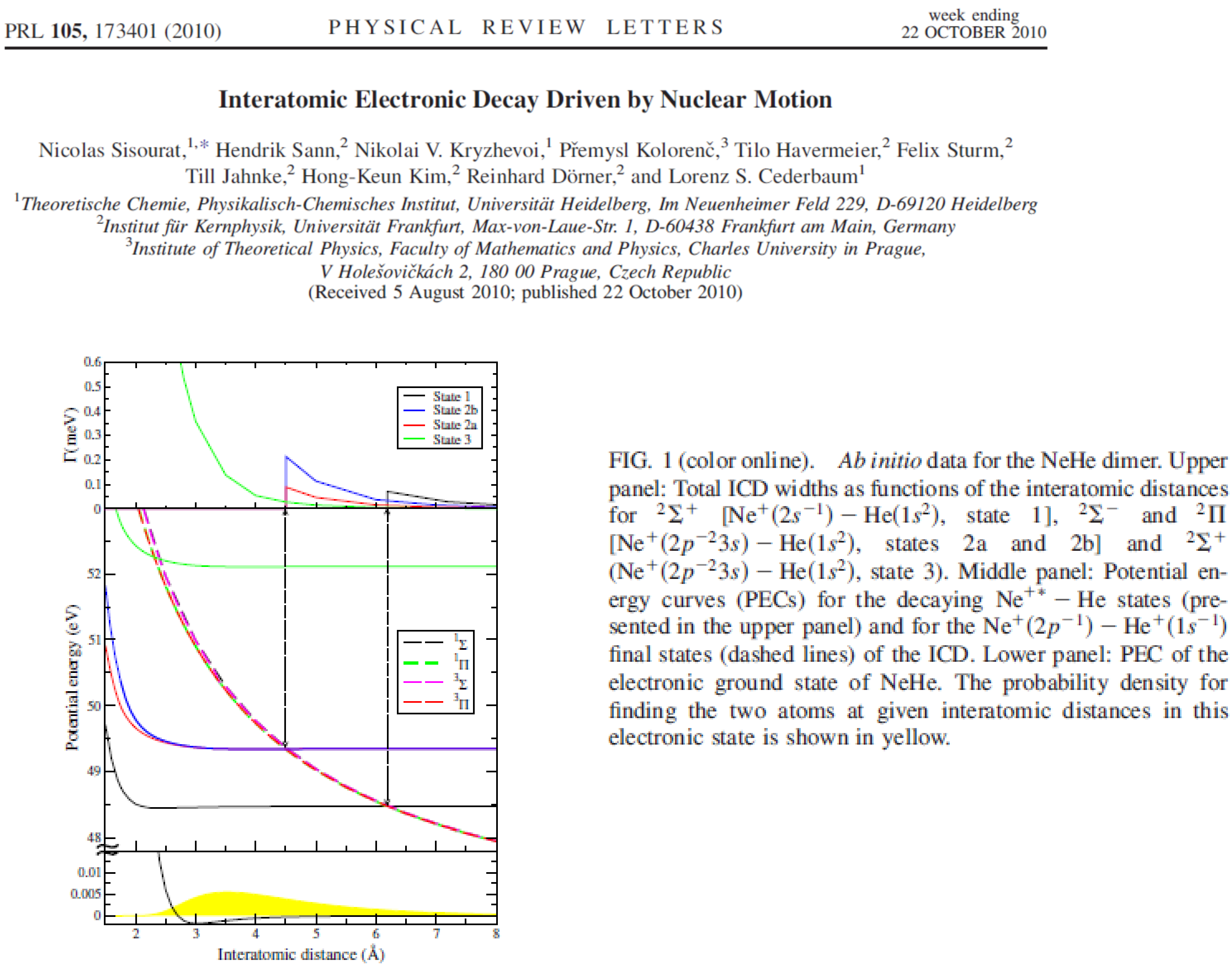

PRL **105,** 173401 (2010) PHYSICAL REVIEW LETTERS week ending 22 OCTOBER 2010

Interatomic Electronic Decay Driven by Nuclear Motion

Nicolas Sisourat,[1,*] Hendrik Sann,[2] Nikolai V. Kryzhevoi,[1] Přemysl Kolorenč,[3] Tilo Havermeier,[2] Felix Sturm,[2]
Till Jahnke,[2] Hong-Keun Kim,[2] Reinhard Dörner,[2] and Lorenz S. Cederbaum[1]
[1]*Theoretische Chemie, Physikalisch-Chemisches Institut, Universität Heidelberg, Im Neuenheimer Feld 229, D-69120 Heidelberg*
[2]*Institut für Kernphysik, Universität Frankfurt, Max-von-Laue-Str. 1, D-60438 Frankfurt am Main, Germany*
[3]*Institute of Theoretical Physics, Faculty of Mathematics and Physics, Charles University in Prague,*
V Holešovičkách 2, 180 00 Prague, Czech Republic

(Received 5 August 2010; published 22 October 2010)

FIG. 1 (color online). *Ab initio* data for the NeHe dimer. Upper panel: Total ICD widths as functions of the interatomic distances for $^2\Sigma^+$ [$\mathrm{Ne}^+(2s^{-1}) - \mathrm{He}(1s^2)$, state 1], $^2\Sigma^-$ and $^2\Pi$ [$\mathrm{Ne}^+(2p^{-2}3s) - \mathrm{He}(1s^2)$, states 2a and 2b] and $^2\Sigma^+$ ($\mathrm{Ne}^+(2p^{-2}3s) - \mathrm{He}(1s^2)$, state 3). Middle panel: Potential energy curves (PECs) for the decaying $\mathrm{Ne}^{+*} - \mathrm{He}$ states (presented in the upper panel) and for the $\mathrm{Ne}^+(2p^{-1}) - \mathrm{He}^+(1s^{-1})$ final states (dashed lines) of the ICD. Lower panel: PEC of the electronic ground state of NeHe. The probability density for finding the two atoms at given interatomic distances in this electronic state is shown in yellow.

Summary

Promoting molecule into excited state

Time evolution on single PES

Population transfer between electronic states

Coupling to continuum

Follow up dynamic

Acknowledgement

Experiment

U. Hergenhahn, MPI Garching
B. Winter, BESSY Berlín

Theoretical Photodynamics Group

Daniel Hollas
Jan Chalabala
Eva Muchová

Theory

Nikolai Kryzhevoi, Heidelberg
Lenz Cederbaum, Heidelberg
Nicolas Sisourat, Paris